Automated verticality alignment system for a Vibro lance

Final year dissertation report

Master of Science in Mechatronics system engineering

Lancaster University
Faculty of Applied Sciences
Engineering Department

Company

Bachy Soletanche LTD
Henderson House
Langley Place,
Higgins Lane,
Burscough, L40 8JB

Report by: Stephen Ako

Acknowledgements

I would like to thank my supervisor Essam Eldin Mohamed Shaban (Engineering department Lancaster University) for his valuable guidance and keen interest in my project.

I would also like to thank my company Bachy Soletanche LTD for support and offering me a chance to reach this academic level and achievement.

Abstract

The aim of the project is to design and develop a control device for monitoring the verticality of a vibro-lance. A vibro-lance is a vibrating probe used in ground improvement techniques to penetrate soft ground conditions with the aid of vibrating forces within the probe. There are a number of ways to manipulate the probe and in this research project the probe will be suspended from the arm of a hydraulic excavator (using the pendulum effect). The Vibrating probe suspended from the excavator arm is driven into the soft ground manually by the operator at the controls of the excavator. The way in which the vibrating probe is suspended from the arm of the excavator allows the probe undesirable rotation about its pivoting point. This movement of the probe calls for the operator to continuously manipulate the excavator arms to correct the verticality of the probe as it rotates out of plumb. The optimum penetration would be a fast movement of the 2 to 3 arms of the excavator, such that the vibrating probe stays vertical at all times while quickly moving up and down inside the void.

The report will research various topics such as, angle sensors to monitor the kinematic position of the excavator arm. Inclinometers that measure the inclination of the vibrating probe, inclinometer that measure the inclination of the excavator body so to obtain an absolute reference between the probe and the excavator arm. The system will also need some sort of intelligent software that can manipulate the excavator arms to counteract any deviating movement of the vibrating probe.

Table of content

List of figures

List of Tables

1.0 Introduction

This section of the report will give a brief outline of ground improvement techniques used in Vibro compaction methods, allowing the reader to gain an appreciation of the overall concept.

Ground condition can be improved or strengthened when it is compressed to reduce the voids between the particulars that make up the strata. This improvement can be achieved by means of a vertical vibration poker inserted into the ground. The vibration within the poker is created by the rotation of an eccentrically weight, this can be driven by either an electric or hydraulic powered motor. The Vibro-lance's head is fitted with a finned wear shield which gives protection and minimises rotation in the ground.

1.1 Vibro-compaction

Vibro-compaction is a ground improvement method used effectively in granular soils. The vibrating probe is lowered into the ground and penetrates downwards under its own self weight; as it travels the surrounding soil is compacted. This compaction of the surrounding soil can be up to a distance of about 2.5m from the probe. As the vibroflot penetrates the granular soils it produces a cavity that is subsequently filled with gravel. This infill of gravel can be fed either from the top of the hole or from the bottom of the flot using a bottom fed vibroflot design. During the compaction of the gravel infill the vibroflot is retracted from the void in incremental steps of around 500mm. Once the 500mm void has been filled with the infill gravel the vibroflot is lowered to compact the lose material. This procedure is repeated until there is adequate stone compaction and column the size has been achieved.

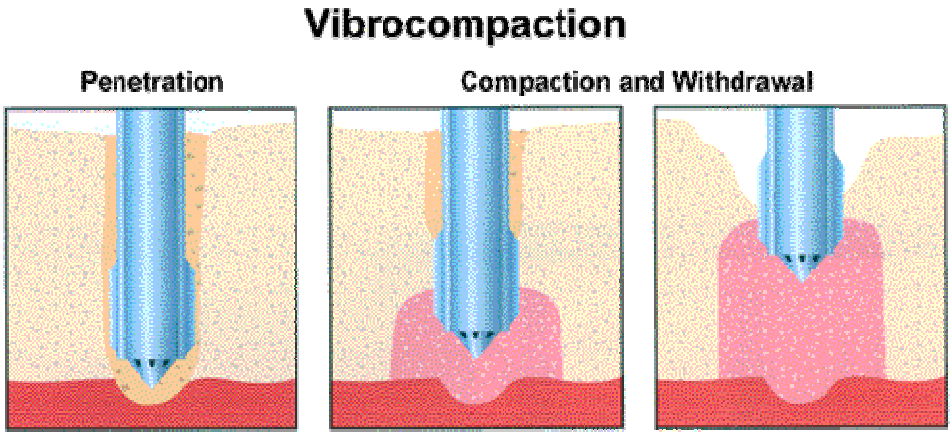

Figure (1) Vibrocompaction utilising a bottom discharge method of gravel infill [1]

1.2 Vibro-flotation

Vibro-flotation is the name given to the procedure where the probe is fitted with water jets. These jets are used to assist the penetration of the vibrating probe into the ground. The water jets are normally fitted to the underside of the probe, in this instance the probe is called a vibrofloat. The water jets are employed to assist the compaction of fine sandy materials. Once the required pile depth is reach the water pressure is reduce while the stone infill is added. The stone column is constructed using the same methods as outlined in section (1.1).

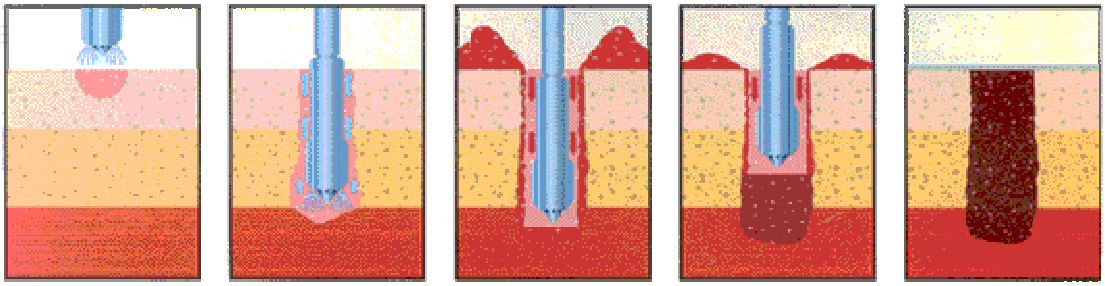

Figure (2) Vibrofloat utilising water jets to aid soil compaction [1]

There are many different methods adopted for installing stone columns using a vibro lance, this report will briefly describe the method of hanging the vibro lance from the arm of an hydraulic excavator.

Figure (3) the vibro lance is connected to the excavator arm and hangs like a pendulum from the machine. The ballast weight of the machine is removed and replaced with an electric power pack for the source of power for electric vibro lance. The machine operator manipulates the poker with movements in this case from the two jointed excavator arm. The vibrating poker penetrates the soft ground under its own weight and vibrating force from the probe tip.

Figure (4) highlights the effects of the incorrect vertical compensation of the hydraulic excavator arms. It is imperative the operator is skilled to keep the vibro lance straight while penetration of the ground is taking place. Any deviation from the vertical will generate undesired stress on the rubber isolate that connects the vibrating probe to the vibro lance extension shaft.

.

Figure (5) highlights the location of the rubber isolator; the yellow horizontal marking is an indication for the reader to locate the isolator position in figure (3) pictured above.

2.0 Viewpoint analysis

To ensure the right design approach for the automated vertically alignment system, a viewpoint analysis was undertaken.

Viewpoint analysis is a process that recognises and suggests that a system should be described from a number of different viewpoints. Bubble diagrams are normally constructed in a brainstorming session where users and system designers suggest possible viewpoints. The first step in the viewpoint analysis is to identify possible viewpoints. A convenient way of expressing a set of viewpoints is to use a viewpoint bubble diagram, which is a simply way for the collection of viewpoint names. Obviously, the more people involved in the brain storming exercise, will relate to how big the bubble diagram will grow. The different variety of subjects highlighted will also relate to the different types of people involved in the brain storming exercise. Following the viewpoint analysis it is possible to highlight the different views suggested from people of different fields and back grounds. The designer could paint a different picture to the system design than an end user or an accountant may do. Figure (6) shows a schematic diagram of the views outlined following the viewpoint analysis all the main area to manufacturer and design the control system were addressed.

2.1 Viewpoint bubble diagram

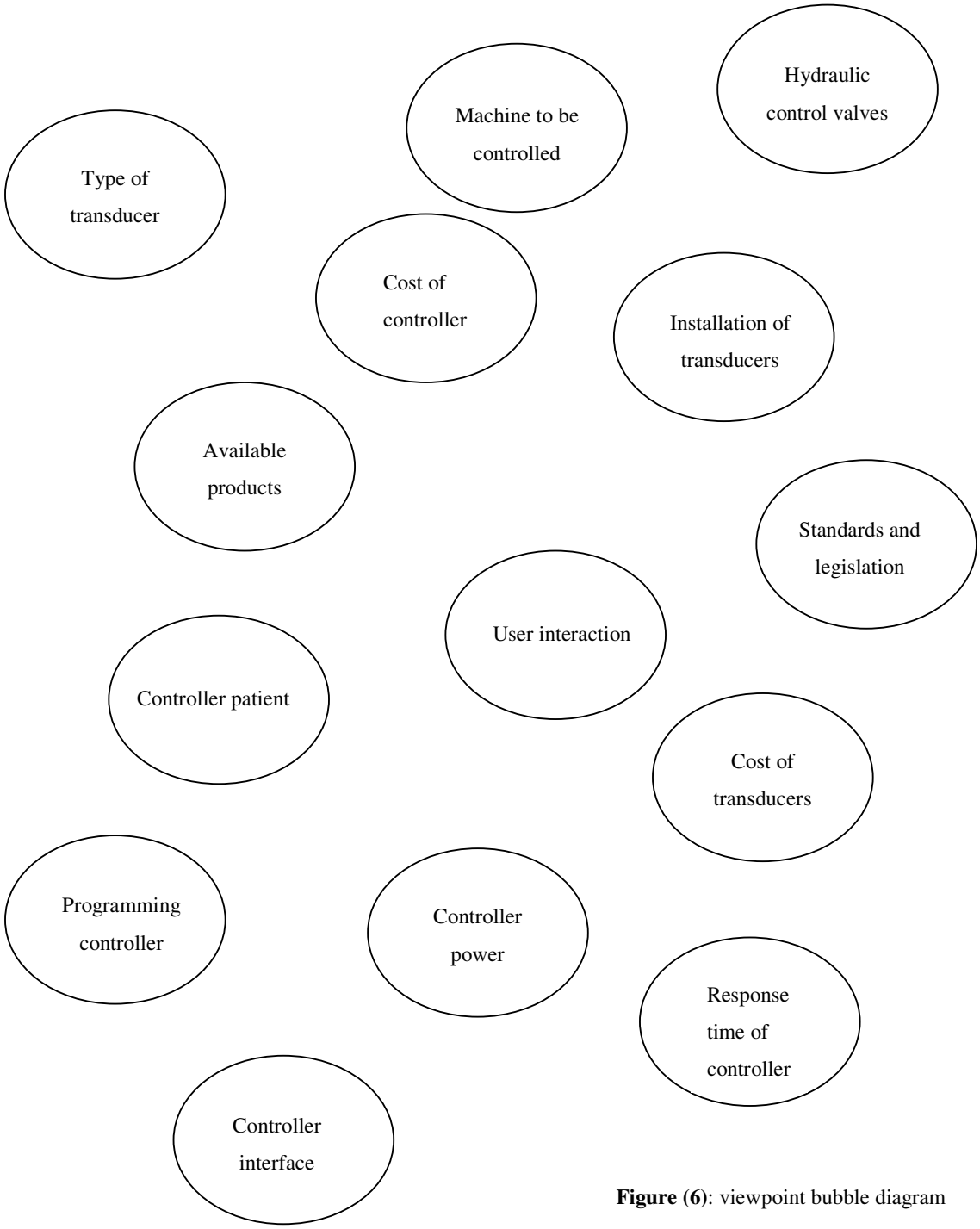

Figure (6): viewpoint bubble diagram

Once the brain storming exercise is complete, the information is then separated into smaller groups and the functional viewpoint chart constructed. From this chart the detailed information needed to design the vibro verticality controller was highlighted. The next stage in the design process is functional analysis and modelling.

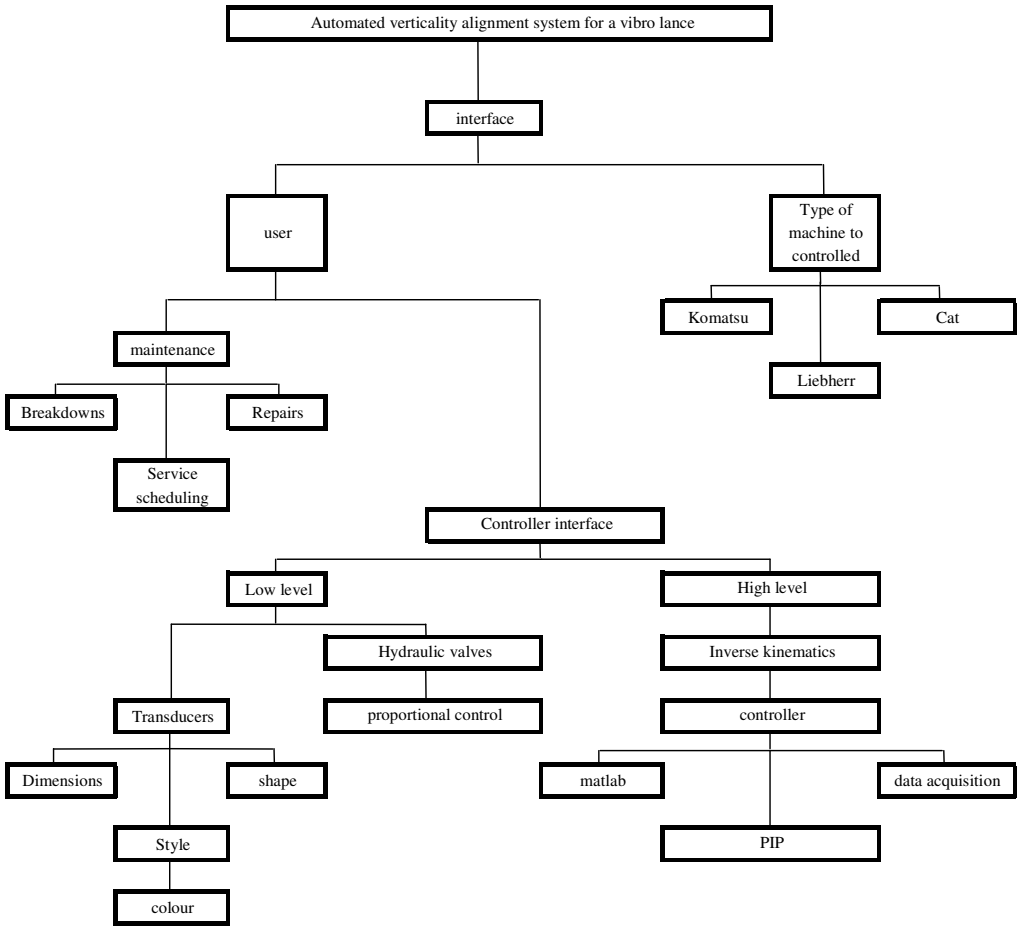

Figure (7): viewpoint structure chart

2.2 Functional analysis and modelling

There are many ways to model a process; in this report the **'Demarco'** modelling method will be investigated.

Demarco modelling: is a method of diagrammatically representing a design process. The model is made up of circles and squares. The square objects are like banks or vendors and circles highlight processes that perform transactions. Between the squares and circles are two different types of connecting lines. Solid lines represent data flow, where lots of data can flow between the objects. Whereas, dotted lines are control lines or control signals. The aim of the control signal is to send information to the 'Data Dictionary'. Here the information can be translated to give a complete and unambiguous command interpretation. The first diagram in the sequence of **'Demarco'** modelling is the context diagram. This top level diagrammatic representation of the controller highlights the main inputs and outputs needed to achieve correct verticality alignment of the Vibro probe.

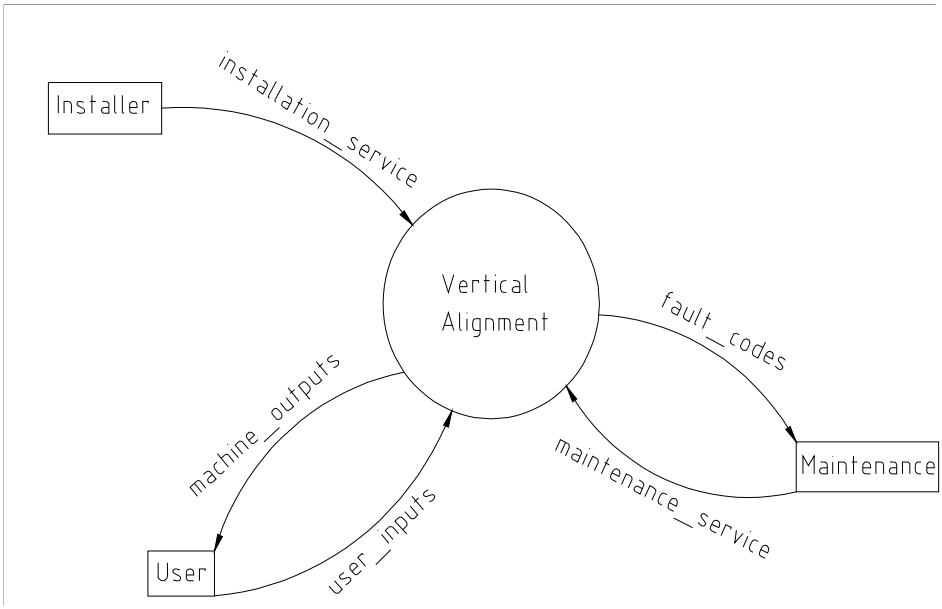

Figure (8) Context diagram

Installation_service:	programming the high level controller
Machine_output:	correct verticality and speed of Vibro lance
User_inputs:	joystick movement of the hand controllers in cab
Fault_code:	coded output number to aid the operator to detect the fault
Maintenance_service:	rectify fault, update system

The next stage in the **'Demarco'** modelling process is to illustrate the different part processing divisions **(level '0')** needed to produce the verticality control system. This report will highlight the proceeding stage **(level '1')**. Here the actual process will be exploded to show the different types of inter processing needed to produce the desired controller output.

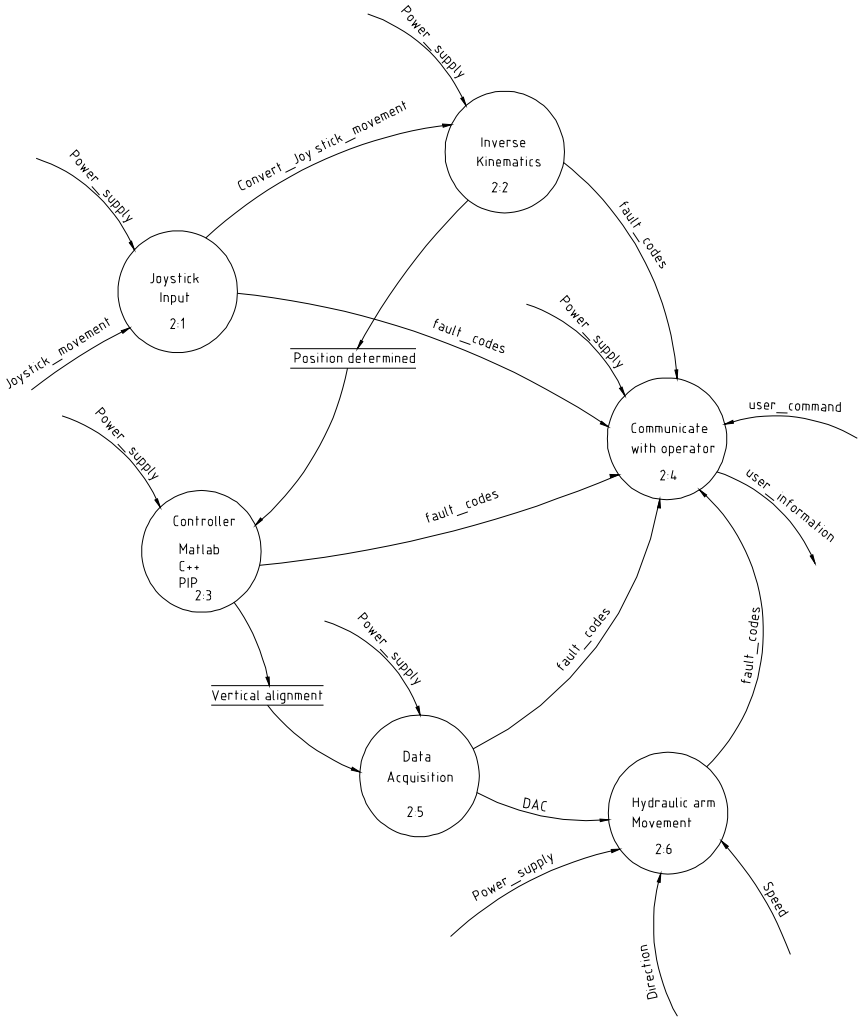

Figure (9) level '1' dataflow for the automated verticality system for a Vibro lance

Key for level '1' dataflow diagram

2:1 while the power supply is on, the processor will convert the joystick movement into binary numbers for processor **2:2** to read. The processor will also send a message to the operator confirming it can interpret the joystick input. A correct reading will be confirmed via the LCD.

2:2 while the power supply is on, the processor will determine the actual position of the excavator arm holding the Vibro lance. The operator is given the X, Y and Z co ordinates of the Vibro lance via the LCD.

2:3 while the power supply is on, the processor will determine the controller output.

2:4 while the power supply is on, the processor is capable of accepting external commands and communicating with the operator.

2:5 while the power supply is on, the processor **2:5** converts (DA) digital to analogue and (AD) analogue to digital from and to the hydraulic arm proportional control valves and positional transducers.

2:6 while the mains power is on; the processor converts all of the inputs to produce movement of the hydraulic excavator arm.

2.3 Sensitivity analysis

System sensitivity analysis enables the design engineer to identify key processes with respect to the system performance. The analysis measures the impact on the projects outcomes after changing one or more key input values about which there is uncertainty. For example, a pessimistic, expected, and optimistic value might be chosen for an uncertain variable. Then an analysis could be performed to see how the outcome changes as each of the three chosen values is considered in turn, with other things held the same. In engineering economics, sensitivity analysis measures the economic impact resulting from alternative values of uncertain variables that affect the economics of the project. Sensitivity analysis can reveal or predict how the verticality controller may react if the input values are not what is expected. Table (1) lists the six sub processes and there sensitivity value.

Data flow	**Receiving processor**	**sensitivity**
Joystick input	2:1	⊕
Inverse kinematics	2:2	⊕
Power_supply	2:1, 2:2, 2:3, 2:4, 2:5 and 2:6	∇
Controller	2:3	⊕
Fault_code	2:4	∇
User_information	2:4	∇
User_command	2:4	⊗
Data acquisition	2:5	⊕
Hydraulic arm movement	2:6	⊗

Table (1) process sensitivity table

Table (1) key

⊕ very sensitive
∇ insensitive
⊗ Sensitive

2.4 Statement of requirements

Based on the information gather (viewpoint analysis, functional modelling and sensitivity analysis), it is now possible to arrive at a statement of requirements for the profitable design and manufacture of the verticality control system. It is seen from table (1) there are four main areas to direct resources.

1. Joystick input
2. Inverse kinematics
3. Controller
4. Data acquisition

These four topics have been highlighted as being the ones that could cause success or failure of the project. More time must be allocated for the development of the four sub processors. This time can be spent improving or removing the possibility of deviation from the expected inputs and outputs.

3.0 Controller hardware

There are a number of ways to monitor the joint angles of the excavator arm,

1. LVDT fitted to hydraulic cylinders of the excavator arm
2. RVDT installed directly on the joint its self
3. Inclinometers

A brief description of each application is outline below.

3.1 (LVDT) Linear Variable Differential Transformers

The device can be fitted internally or externally to hydraulic cylinders they would provide linear position measurement of the cylinder rod. They have a non-contacting design which provides high reliability with no deterioration in performance. This absence of physical contact between the moving parts within the LVDT means the device is frictionless when in operation and therefore no parts to wear out. The measuring device has infinite resolution and could respond to the minute linear displacement of its core which would be attached to the cylinder rod; this in turn would generate a voltage output proportional to the excavator joint angle for which the cylinder was manipulating. The units have many different internal designs. Basically they are an electromechanical device which consists of a primary coil, a ferrous moveable core and two secondary coils. The core is situated between the primary coil and the two secondary coils. This allows a magnetic flux path proportional to the AC voltage applied to the primary coil to be transmitted to the secondary coils. The secondary coils are connected in series, when the core is in a central position the output voltage is zero. When the core travels off in one direct the output voltage becomes (+ve) positive. When the core travels in the opposite direction the output voltage becomes (-ve) negative. See figures (3) for a simple schematic diagram of an AC-LVDT principle. Using simple electronics the AC output voltage from the secondary coils can be converted to a simple DC voltage or a 4-20ma signal.

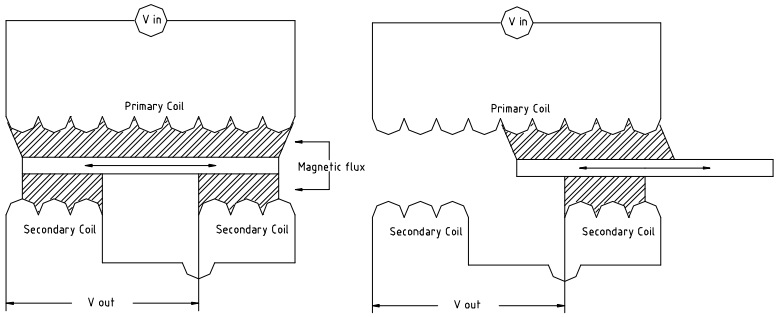

Figure (10) Principle of an AC powered LVDT sensor [2]

3.2 (RVDT) Rotational Variable Differential Transformers

The design principle of the RVDT is basically the same as that outlined above in section 2.1. The difference in design is way in which the iron is moved. With the (LVDT) the core is moved linearly to generate a voltage output whereas the core is rotated within the (RVDT) transformer design to generate its voltage output see figure (4)

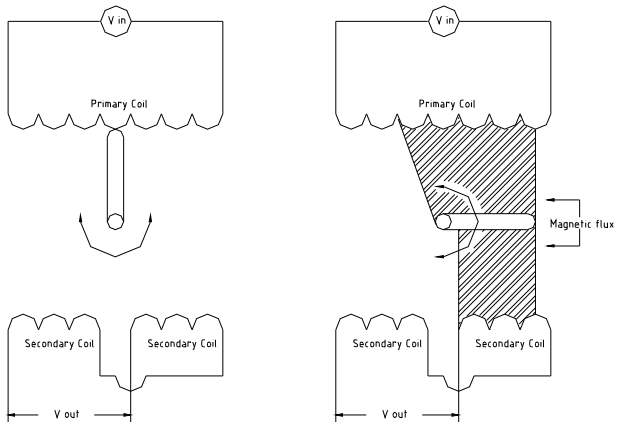

Figure (11) Principle of an AC powered RVDT sensor [2]

This type of sensor design would locate directly on the excavator arm joints and its output voltage is proportional to the joint angle.

3.3 Inclinometers NG' range'

This type of transducer is a liquid based sensor fitted with integrated sensor electronics. The sensor can be supplied with measuring ranges of ±10º, ±20º, ±60º, ±80º and 360º monitoring capabilities. The input for this type of sensor is 24vDC capable of producing a 4-20ma current output proportional to the angle of the sensor. The measuring principle of the inclination sensor is obtained by placing two electronic probes within a capacitive liquid. In the central position (0º) tilt both probes will share the same volume of liquid therefore generating a central output i.e. in this case 12ma. As the sensor begins to rotate the liquid inside the unit tilts under the force of gravity therefore unbalancing the shared of the capacitive liquid thus changing the output signal. See figure (8) for the NG4/S Inclinometer fitted to the excavator boom.

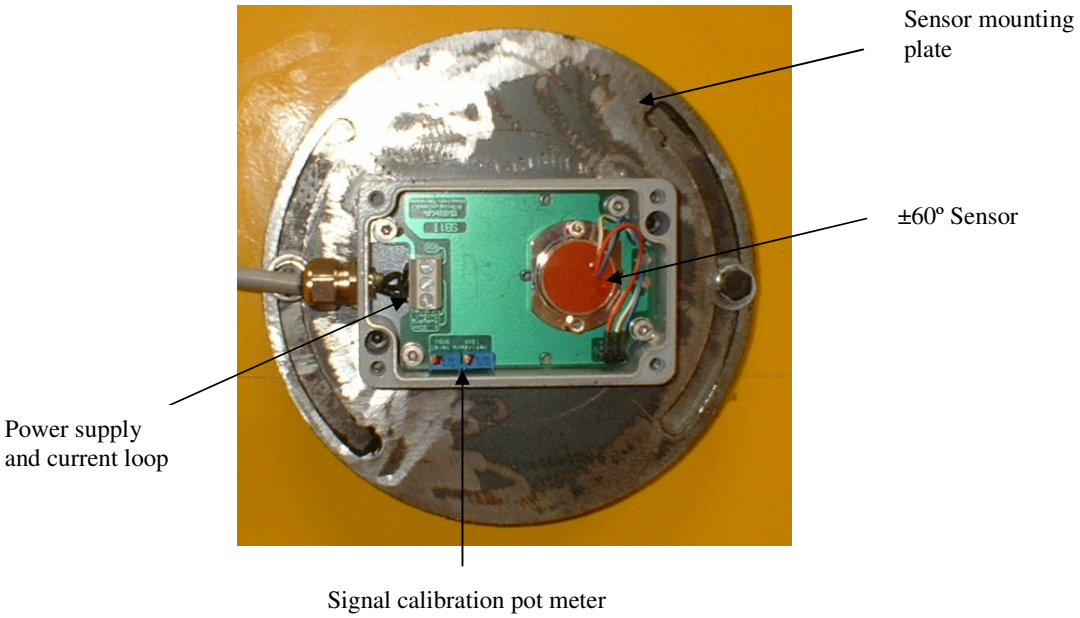

Figure (12) NG4/S Inclinometer ±60º measuring range [3]

3.4 Selecting the sensor

1. **Sensor measurement technique:** the sensors will fit the arm and boom for the monitoring of each individual joint movement respectively. The selection of a linear transducer will invoke a calibration to translate linear movement to a rotational joint movement.
2. **Disturbance:** this feature is found in almost every small to medium sized excavator. When the operator of the machine requires crowd force to over come obstruction in the digger strata they use all available machine power to push the vibro lance into the ground. The Komatsu PC 240 LC is capable of generating enough downward arm force to lift the front of the excavator from the ground. This undesirable movement of the base carrier pictured in figure (9) is registered by the sensors monitoring the relative joint angle, in turn affecting the inverse kinematics and therefore the controller output. A sensor capable of monitoring the joint absolute angle in this case is more desirable.
3. **Range:** The measuring range of the sensors must span the full movement of both joints needed to produce the required trajectory.
4. **Installation:** the method and time needed for the sensor installation will have a large impact on the overall controller design and flexibility. The main feature in the controller design is the installation process which is done with little or no alterations to the excavator. The sensor design can have no limitation as to what excavator arm cylinder or joint it is fitted to.
5. **Availability:** If the sensor was to malfunction, what is the cost of a typical repair, maintenance, or even a sensor replacement? In the event of reordering a sensor due to malfunction the supplier must be capable to react with a short delivery time for the sensor replacement.
6. **Cost:** In the preliminary sensor specification the component cost has a low rating compared with the other sensor parameters. This feature only gains strength once the controller design has been evaluated.

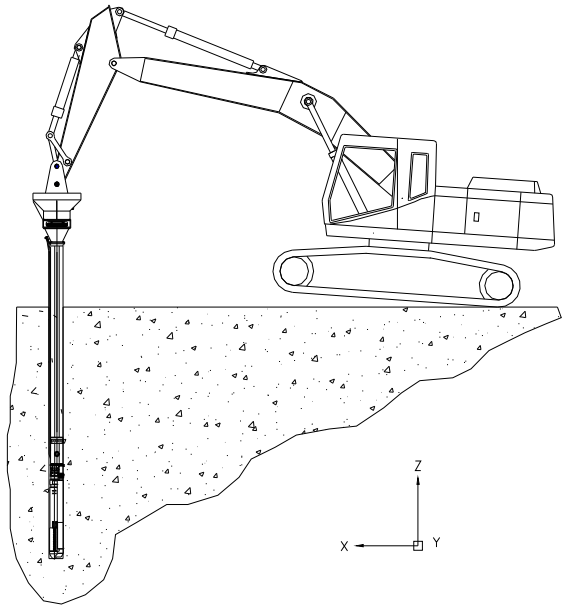

Figure (13) Pictures the PC 240 LC excavator lifting when producing arm crowd.

Table (2) features the sensor parameters with overall rating. The inclinometer came out with the highest rating and was therefore selected to monitor the excavator arm joint movements

Sensor parameter	**Possible rating**	**(LVDT)**	**(RVDT)**	**Inclinometer** NG4/S ±60º
Sensor measuring technique	5	5	5	5
Disturbance	5	0	0	5
Range	5	5	5	5
Installation	5	0	1	5
Availability	5	1	2	5
Cost	5	1	2	5
Overall sensor rating	30	12	15	30

Table (2) sensor rating

Figure (14) above side profile of the PC 240 LC, below left boom sensor, below right arm sensor

3.5 Calibration of the sensors

This section of the report looks at the simple method used for the calibration of the excavator arm sensors. The sensors work on a single axis of ±60° which enables the units to output a linear signal of 4-20ma. The way in which the sensors were to be calibrated made the mounting of them on the excavator arm simple. There was no need for precision alignment of 0° sensor orientation with 0° of the boom or arm joint axis. All that was needed was to ensure the sensor measuring range spanned the joint movement needed for the overall trajectory figure (10) show the max and min joint movement. Once the sensors were mounted several joint signal readings were taken and logged along with there corresponding joint angles found using an angle meter (*Starrett Exact, angle meter, Athol, MA 01331 USA magnetic base*).

Figure (11) and (12) are the calibrated sensor input/output response, using the expression for a straight line (y=mx+c) a relationship of the sensor angle (degrees) and output sensor signal (decimal) could now be related. Using the information given by the graph the angle of the boom and arm could now be found for any input signal.

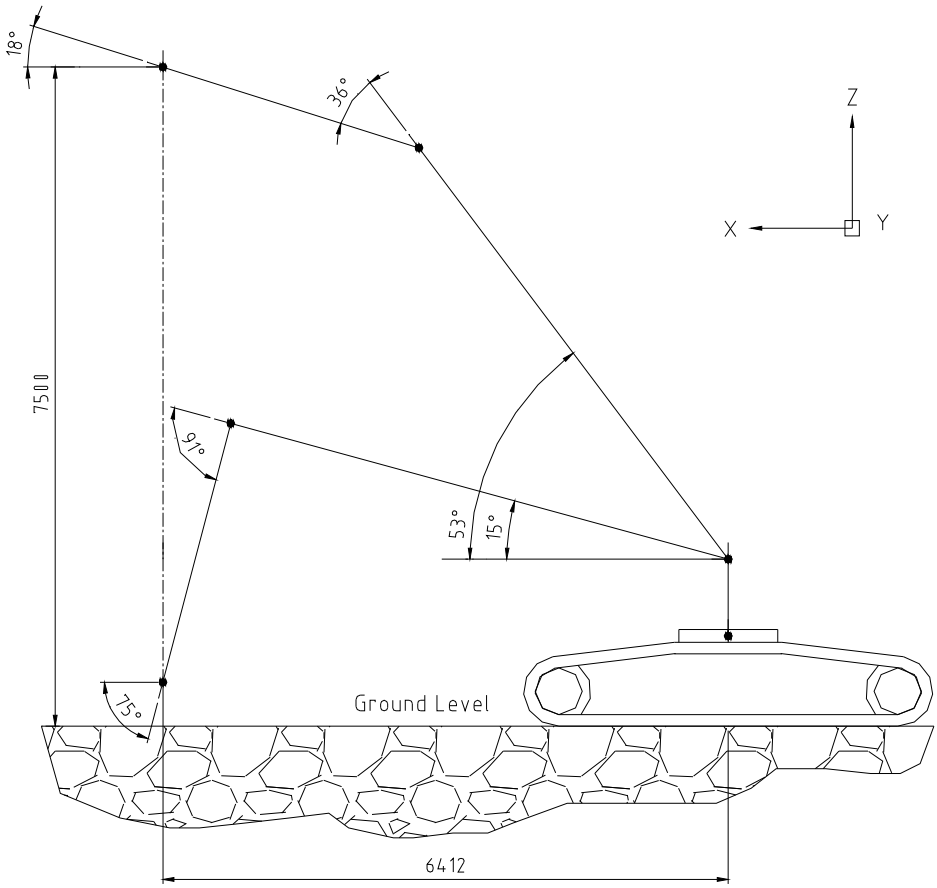

Figure (15) the initial and end position of the vibro pivotal relating the boom absolute sensor span angle of 53° and arm absolute sensor span angle of 93°

Figure (16)
Boom Joint angle (deg)
(Y = 0.0769x + 71.703)

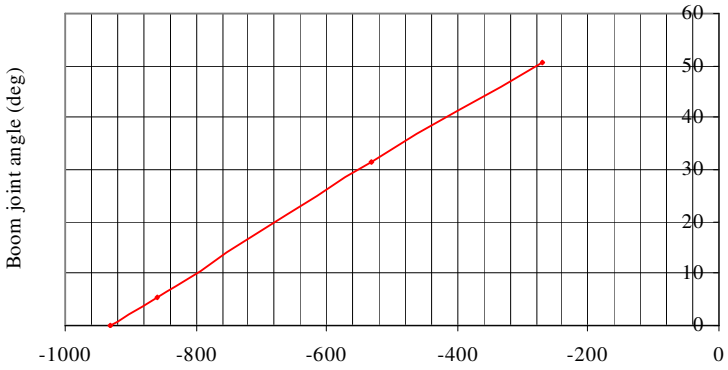

Figure (17)
Arm joint angle (deg)
(Y = 0.0748x + 33.225)

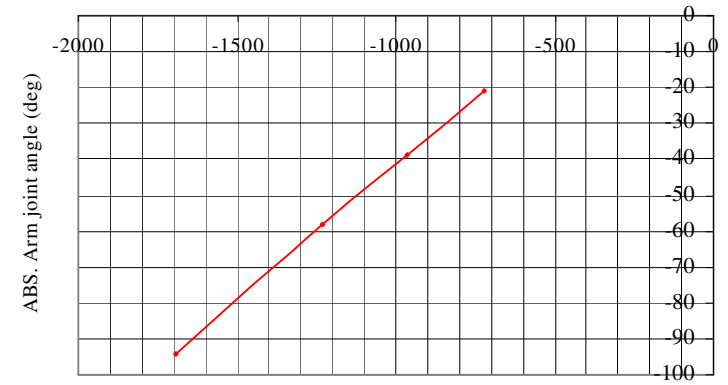

3.6 Hydraulic control

After study the hydraulic circuitry for the Komatsu PC 240-7 LC [1] it became apparent to replace the existing boom and arm hydraulic control values for proportional control wouldn't be good design practise. It would be more economical to simply incorporate a few extra control valves and hydraulic circuitry.

3.7 Proportional control

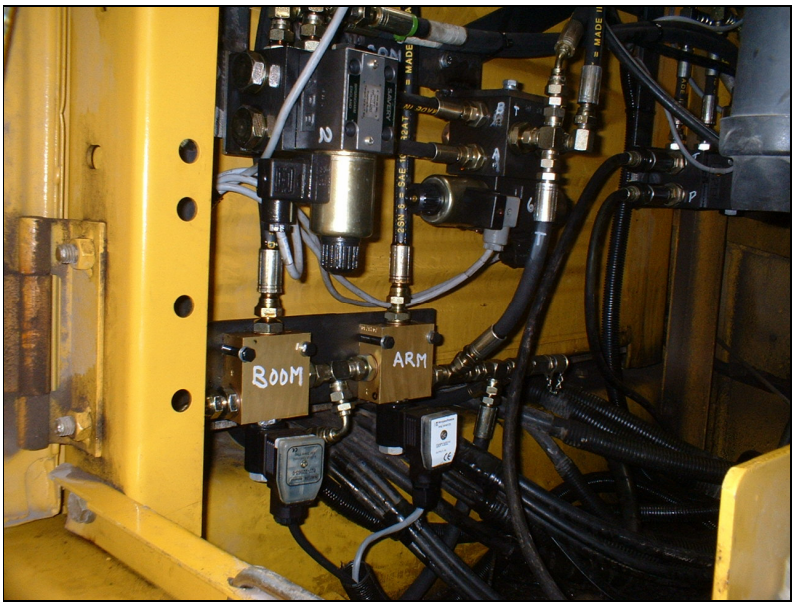

DIN type plug electronics fitted to a 24vDC solenoid make up the neat proportional control valves labelled boom/arm opposite. The electronics are designed to take an input signal of 4-20ma for the proportional control of the directional control valve.

Figure (18) pictures the boom and arm proportional control valves [4, 5]

3.7.1Setting the min/max current

The minimum current needed to open the proportional valves to overcome the weight imposed on the joints from the arm and boom could have been adjusted via adjustable pots located on the DIN plugs. The min bandwidth setting was found by sending small amounts of current to the proportional controller and observing the movement of the joint as soon as the joint moved the min current was logged. The valve max setting was capped to allow the excavator arm to move freely and safely while the research for the controller took place. See the C++ program below for the hydraulic valve calibration program.

3.7.2 C++ valve calibration program

```
#include "struct.h"
Int SELECTOR;
Struct ValveData VALVE[2]
{
 {0,            //ValveRelay          = Value corresponding to the Valve Relay
  3267.0,       //ValveMax            = Max. Drive setting (V) this was restricted for safety      = BOOM
  3100.0,       //ValveDeadbandHi     = Dead band high point to move the boom up
  2047.0,       //ValveMid            = Valve midpoint (neutral)
  3020.0,       //ValveDeadbandLo     = Dead band low point to bring the boom down
  3267.0,       //ValveMin            = Min. drive setting
  0,            //Demand              = Demand coming from joystick in +/-1000
  0,            //Resolved Demand     = Resolved Demand
  0,            //Previous Demand     = Previous Demand
  2047,         //Drive Demand        = Demand to be passed to valves
  19.33,        //Valve_fo            = Proportional Valve Gain
  -0.7,         //Valve_g1            = Plus Valve Gain
  0.67,         //Valve_kI            = Integral Valve Gain},

 {0,            //ValveRelay          = Value corresponding to the Valve Relay
  3267.0,       //ValveMax            = Max. Drive setting (V) this was restricted for safety      =ARM
  2990.0,       //ValveDeadbandHi     = Dead band to move the arm up
  2047.0,       //ValveMid            = Valve midpoint (neutral)
  2970.0,       //ValveDeadbandLo     = Dead band to bring the arm down
  3267.0,       //ValveMin            = Min. drive setting
  0,            //Demand              = Demand coming from joystick in +/-1000
  0,            //Resolved Demand     = Resolved Demand
  0,            //Previous Demand     = Previous Demand
  2047,         //Drive Demand        = Demand to be passed to valves
  45,           //Valve_fo            = Proportional Valve Gain
  -0.1,         //Valve_g1            = Plus Valve Gain
  5,            //Valve_kI            = Integral Valve Gain},
}; // end ValveData
```

The rest of the hydraulic circuitry is made up of shut off, pressures reducing, directional control valves see figure (19) and (20).

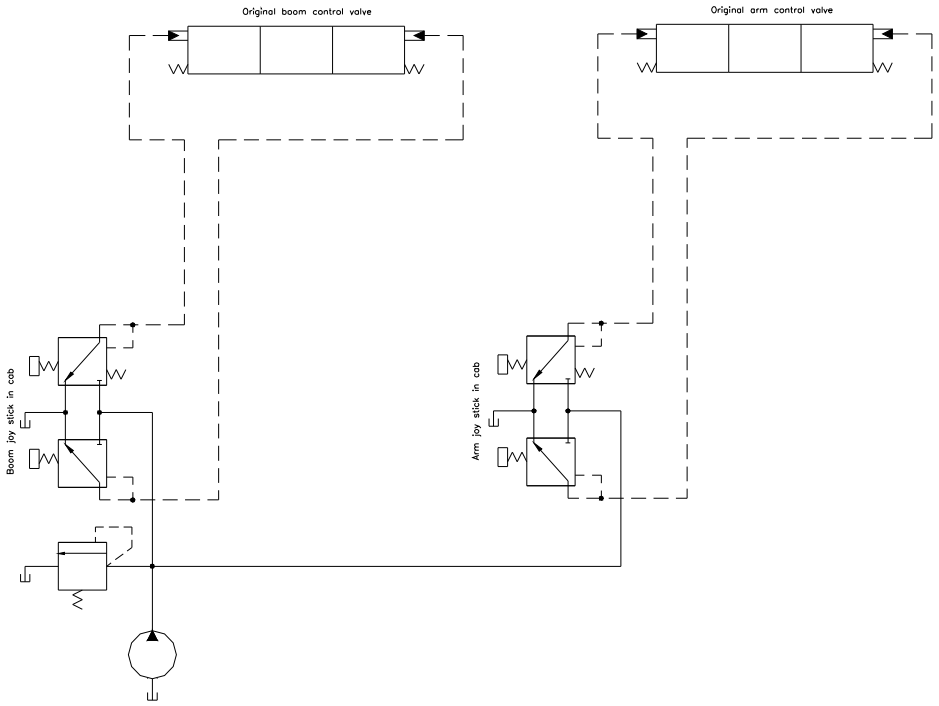

Figure (19) original hydraulic control circuitry

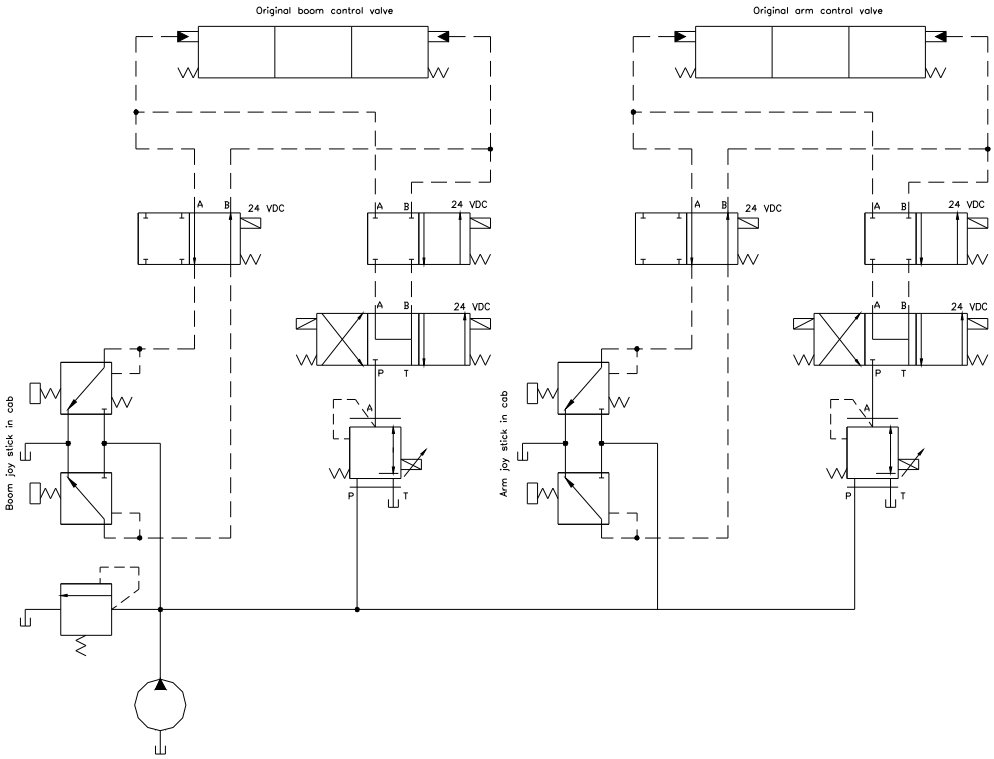

Figure (20) revised hydraulic control circuitry

3.8 Controller joystick

The controller joystick has two functions:

1. direction of the end effector
2. speed of the effector

When the controller is monitoring the trajectory of the excavator arm, both the boom and arm (dipper) movement are synchronised via the controller from the single joystick movement. With the excavator in automatic trajectory mode, the two manual boom and arm (dipper) joysticks are immobilised.

Figure (21) HFX Hand Grip (HG) Joystick [3, 4]

The unit is a rugged design and is engineered to handle the toughest jobs. Conventional uses for the HFX Hand Grip include: construction, farm equipment, forklifts, off-road machinery, lift platforms, tractors and crane applications [3]. The device is light weight, streamline and fits nicely into the cab of the excavator with little fuss. The joystick model chosen is fitted with an internal limit plate which restricts the movement of the joystick handle to movement in the (Y axis only).

The joystick can be supplied with various outputs, for the control of the Komatsu an output 0.25V to 4.75V was used.

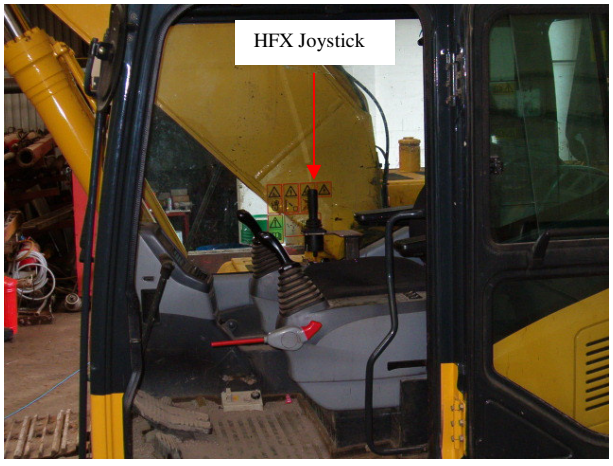

Figure (22) The HFX Hand Grip location in the cab of the Komatsu PC240 LC-7

3.9 Motion controller

The next step in the controller design was to identify a controller capable of receiving and sending information to the chosen sensors.

The pc card/s would need to handle:

1. 2No output proportional control signal = 4-20 (ma)
2. 2No input Inclinometer = 4-20 (ma)
3. 1No Joystick = 0 – 5 (vdc)
4. 4No relays for the directional control of the individual joints

3.9.1 AIM104-MULTI-IO [4]

The AIM104-MULTI-IO is an 8-bit PC/104 module. It incorporates all the features found in standard PC/AT systems and has extra support for embedded applications, additional serial ports, general purpose I/O and silicon disk. The board is supplied with 100MHz CPU, 16MB DRAM, 8MB Flash, which has been pre-configured with Data light's ROM-DOS operating system. The AIM104-MULTI-IO providing 8 opto-isolated digital inputs, two 12 bit (DAC) analogue outputs (Voltage or Current Loop) and 16 single ended or 8 differential 12 bit ADC analogue inputs with a channel conversion time of 500msec.

3.9.2 AIM104-RELAY8/IN8 [4]

The AIM104-RELAY8/IN8 is an 8-bit PC/104 module providing 8 changeover relays, and 8 opto isolated. The power switching rating for the relay contacts is 60W (resistive load). The relays and board layout are designed to switch voltages up to 220v DC (125v AC) and currents up to 1.0A. However the Low Voltage Directive specifies that the product may only be safely used up to 48v DC.

3.9.3 **ACEpc** enclosure [4]

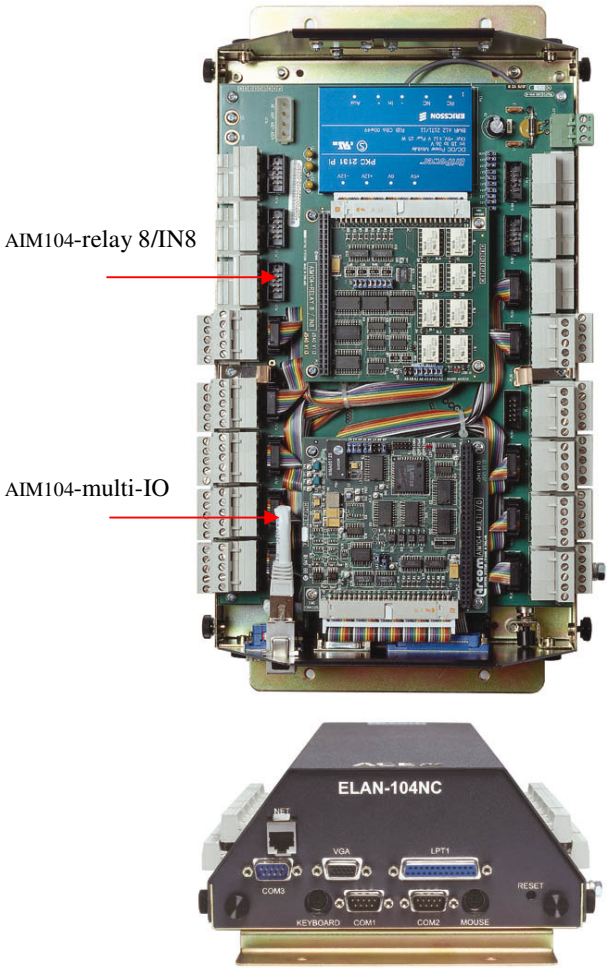

Figure (23) ACEpc enclosure

The AIM104-MULTI-IO and the AIM104-RELAY8/IN8 were installed into this neat enclosure to provide protect for the pc cards. The enclosure provided easy connection for the:

1. Monitor
2. Keyboard
3. Laptop
4. Mouse
5. Power supply
6. The external sensors

The enclosure includes a 100MHz AMD SC400 based ELAN-104NC which offers multiple PC/104 expansion and screw terminal connection for input/output, sensor/actuator coupling.

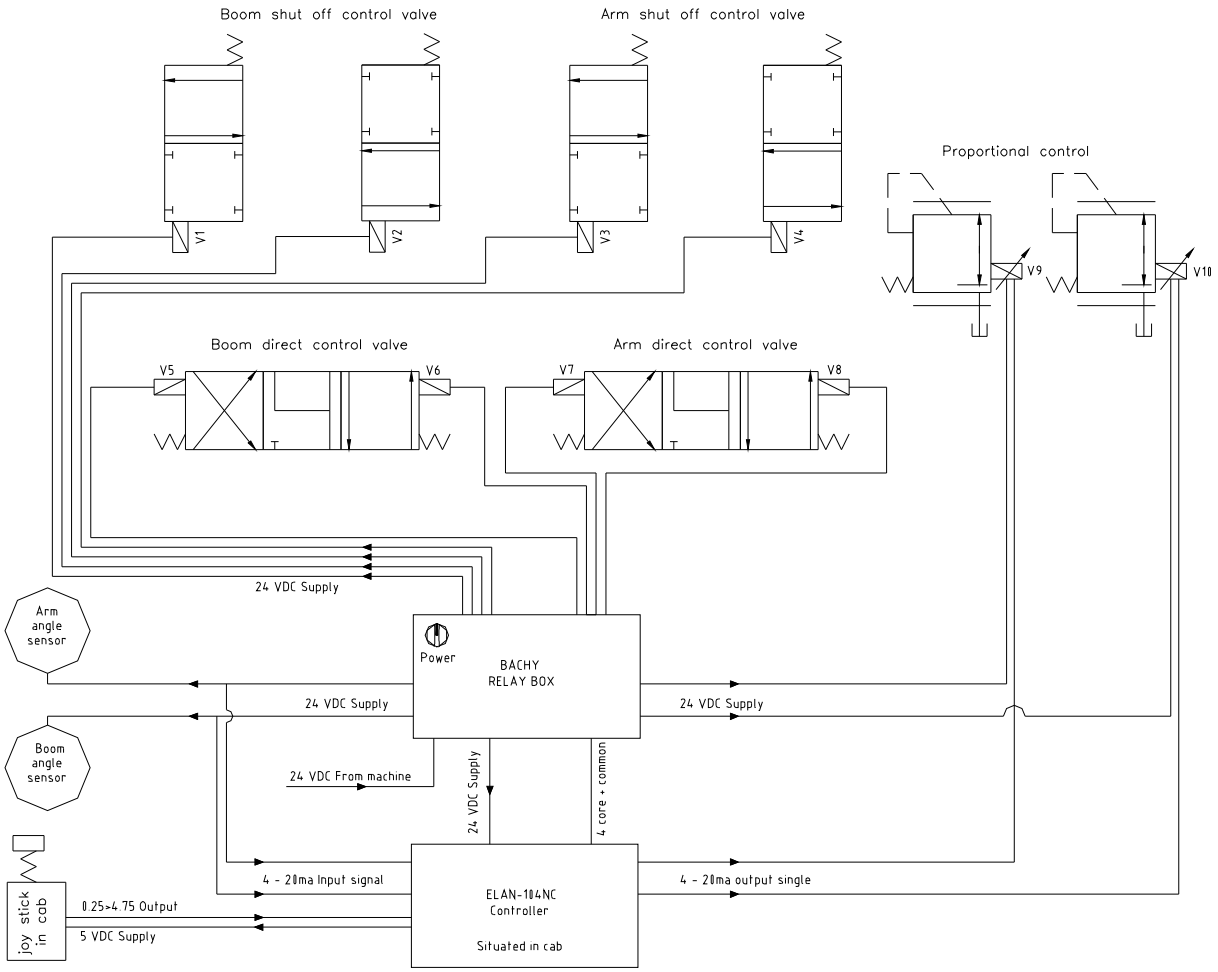

Figure (24) schematic representation of the excavator trajectory control circuit

4.0 Kinematics

To ensure the correct orientation of the Vibro lance, the relationship between the Vibro pivotal axis and the excavator is needed, this is called the kinematic analysis. The analysis is split into two sub-processes, direct and inverse kinematics. This section of the report will explain both processes.

The verticality controller in a nutshell is a process that converts the manually operated hydraulic excavator arm into a semi automated manipulator. The excavator to which the controller shall fit has an arm capable of three degrees of freedom. With the controller switch on and monitoring the Vibro lance verticality, the excavator end-effecter (*the pivotal axis of the Vibro lance*) will be elevated to a typical working height of 7.5 mtrs from ground level (*the overall length of the Vibro lance*). The objective of the controller is to aid the machine operator, in keeping the verticality of the lance as it is vibrated into the ground to a desired depth. The three joy stick movement needed to manipulate the excavator arm in a vertical motion will be replaced by a single joy stick movement. This single joy stick operation by the operator will instruct the controller as to what speed and direct to move the three jointed arm of the excavator. The controller will basically consist of four sub-processes, see fig (25).

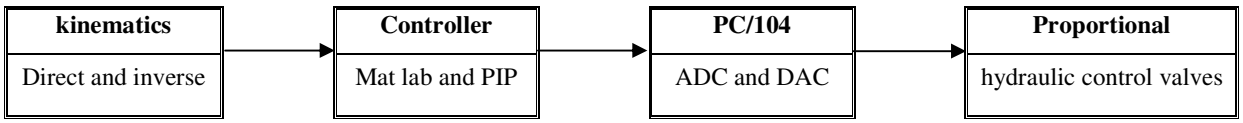

Fig (25) highlights the four main vertical controller sub processes

4.1 Direct kinematics

Direct kinematics is a tool used to find the position, orientation, velocity and acceleration of the Vibro lance pivotal with respect to the orientation of the excavator base. There are two approaches for this technique:

1. Geometry based direct kinematics analysis
2. Co ordinate and vector transformations using matrices

This report is based on the latter process of co ordinate and vector transformations using matrices. A transformation is a process of calculating the relationship of one joint with another, whether it is a rotational or linear movement between the two corresponding joints.

The verticality control system performs rotational movements of the excavator arm joints. This movement of the joints will produce a linear vertical motion in the (Z) axis of the vibro lance as it is manipulated from its start position to the desired. The most appropriate technique to find the position of the pivotal point is to use the **homogeneous transformation matrices** method. The transformation matrix is the relationships between two consecutive joints or co ordinates. The matrix is made up of an orientation matrix and a translation vector.

4.2 The orientation matrix [6]

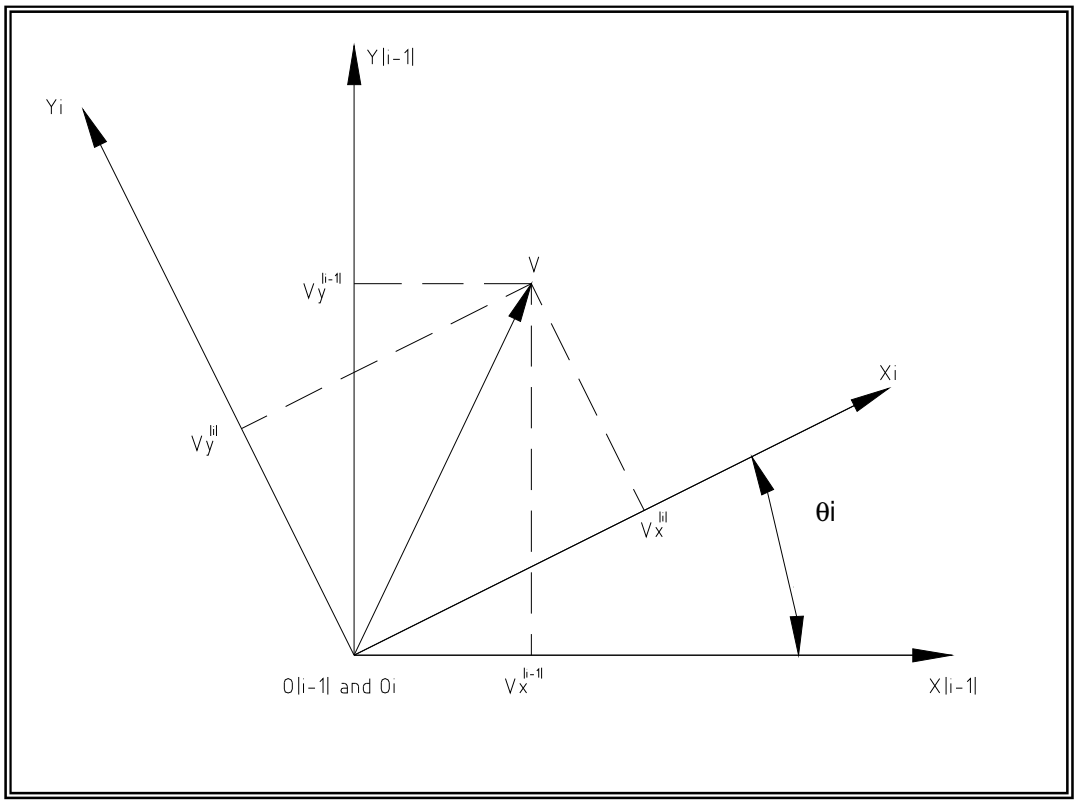

Fig (26) Orientation Matrix

Where O_i is at the origin and the rotational axis relative to $O_{(i-1)}$. The vector component (V) has been rotated through θ_i and therefore an equation expressing the movement of the frame $X_{(i-1)}, Y_{(i-1)}$ with respect to frame X_i, Y_i can be produce.

$$V_x^{(i-1)} = V_x^{(i)} \cos\theta_i - V_y^{(i)} \sin\theta_i \qquad \ldots 1$$

$$V_y^{(i-1)} = V_x^{(i)} \sin\theta_i + V_y^{(i)} \cos\theta_i \qquad \ldots 2$$

Equations (1 and 2) can be re written and expressed in matrix form:

$$\begin{bmatrix} V_x^{(i-1)} \\ V_y^{(i-1)} \end{bmatrix} = \begin{bmatrix} \cos\theta_i & -\sin\theta_i \\ \sin\theta_i & \cos\theta_i \end{bmatrix} \begin{bmatrix} V_x^{(i)} \\ V_y^{(i)} \end{bmatrix}$$ Simplify the above equation and letting:

$$V^{(i-1)} = \begin{bmatrix} V_x^{(i-1)} \\ V_y^{(i-1)} \end{bmatrix} \qquad R_{(i-1)}^{i} = \begin{bmatrix} \cos\theta_i & -\sin\theta_i \\ \sin\theta_i & \cos\theta_i \end{bmatrix} \qquad V^{(i)} = \begin{bmatrix} V_x^{(i)} \\ V_y^{(i)} \end{bmatrix}$$

Then the orientation matrix can be express as:

$$V^{(i-1)} = R_{(i-1)}^{i} V^{(i)}$$

Where:

$R_{(i-1)}^{i}$ Is the rotation matrix describing the orientation of frame O_i with respect to frame $O_{(i-1)}$

4.3 The translation matrix

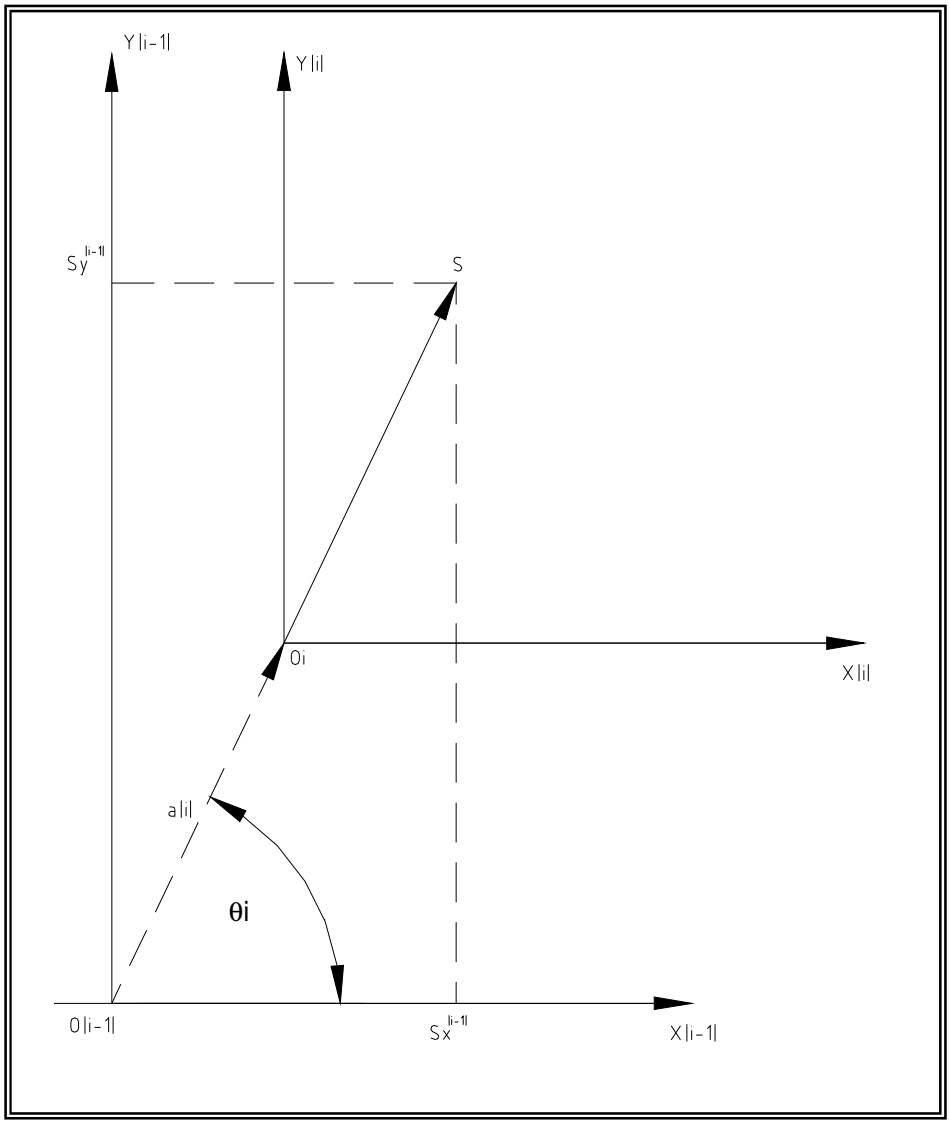

Fig (27) Translation Vector

The translation vector describes linear movement of the axis in the x, y and z planes. Fig (x) highlights a movement of the origin in the x, y plane; therefore the following translation vector equation is produced:

$$P_x^{(i-1)} = a_i \cos\theta_i + P_x^{(i)} \qquad 1$$

$$P_y^{(i-1)} = a_i \sin\theta_i + P_y^{(i)} \qquad 2$$

Equations (1 and 2) can be re written and expressed in matrix form:

$$\begin{bmatrix} P_x^{(i-1)} \\ P_y^{(i-1)} \end{bmatrix} = \begin{bmatrix} a_i \cos\theta_i \\ a_i \sin\theta_i \end{bmatrix} + \begin{bmatrix} P_x^{(i)} \\ P_y^{(i)} \end{bmatrix}$$

Then the translation vector can be express as:

$$P^{(i-1)} = d^i_{(i-1)} + P^{(i)}$$

4.4 The homogeneous transformation matrix

Finally the two above matrices are brought together in order to calculate the overall position and orientation of the translated origin using the homogeneous transformation matrix method. This type of matrix consists of four sub matrices:

$$\left[\begin{array}{c|c} \textit{Rotation matrix} & \textit{Position Vector} \\ \hline \textit{Perspective transformation} & \textit{Scaling} \end{array}\right] = \left[\begin{array}{c|c} R^i_{(i-1)} & d^i_{(i-1)} \\ \hline f & S \end{array}\right]$$

4.5 Denavit-Hartenberg notation rule

Kinematic modelling will identify the relationship between the excavator joints or degrees of freedom. The modelling process will take into account the orientation, length and type of joint (revolute or prismatic). Revolute joint is where the adjacent link is allowed to rotate about the common joint axis. Prismatic joint is a link that allows the adjacent joint to translate linearly along the common joint axis. The first axis of the excavator joint (1) is revolute, allowing the super structure to rotate about the base at a central pivotal point. Joint (2) is also revolute its origin is a distance d_1 along the common z-axis from joint (1) and its axis is rotated +90º about the x-axis, according to the right hand rules of notation. The remaining joints (3) and (4) are also revolute at distance a_2 and a_3 respectively from joint (2) along the x-axis.

Before the Denavit-Hartenberg notation table can be constructed there are four outlined parameters to follow:

1. a_i The distance between $O_{(i-1)}$ and $O_{(i)}$ along the common X-axis
2. d_i The distance between $O_{(i-1)}$ and $O_{(i)}$ along the common Z-axis
3. α_i The right hand notation rule this is the angle between the $Z_{(i-1)}$ and Z_i about the common X-axis
4. θ_i The angle between $X_{(i-1)}$ axis and X_i axis measured about the axis $Z_{(i-1)}$ according to right hand notation rule. For a revolute joint this is always θ_i

Figure (12) shows the fully constraint excavator arm with its joint number and parameters.

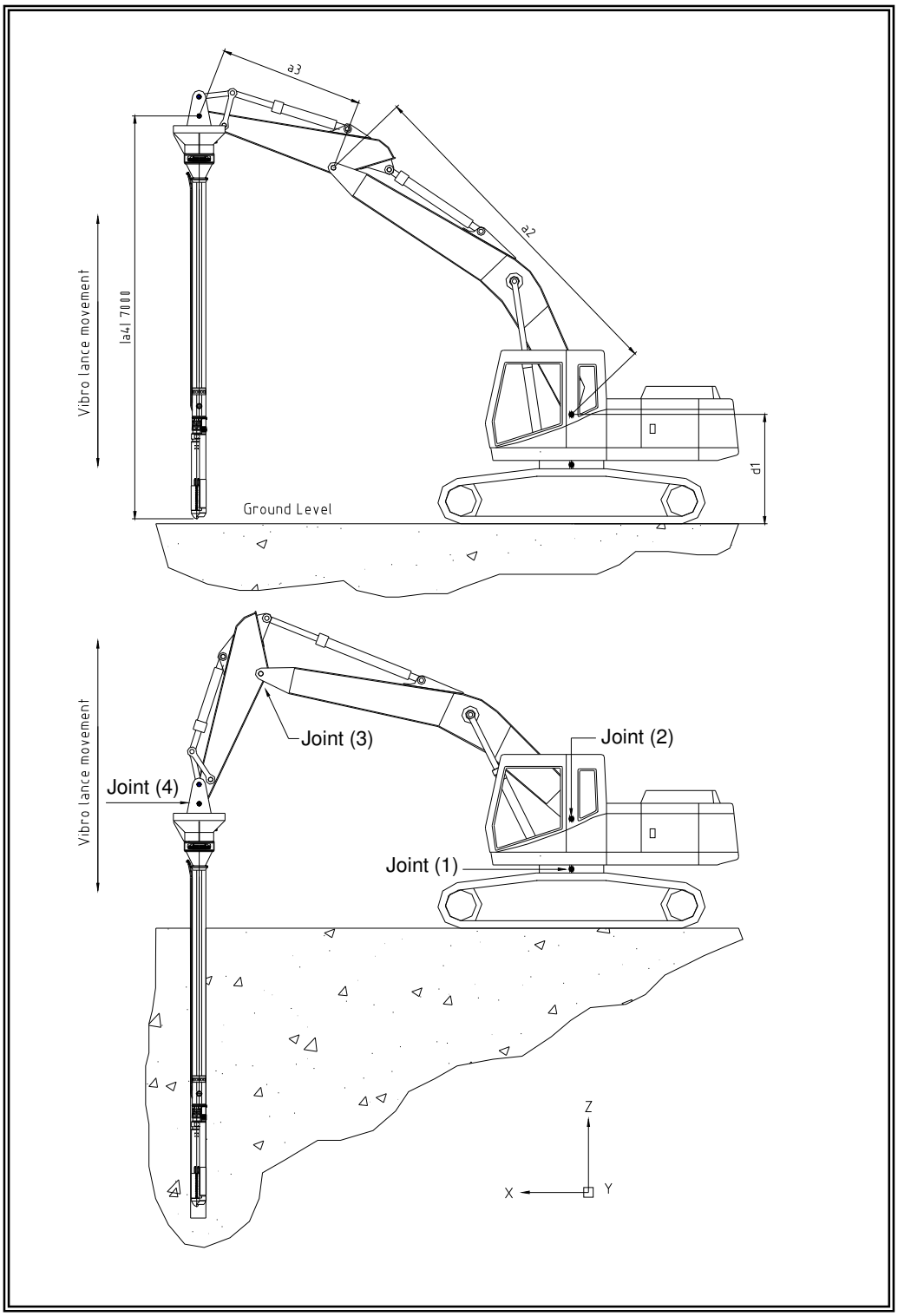

Figure (28) Shows the fully constraint excavator arm with its joint number and parameters

The Denavit-Hartenberg link parameters for the excavator arm are tabulated in table (2)

Joint	Joint Parameters			
	θ_i	d_i	a_i	α_i
1	θ_1	d_1	0	90
2	θ_2	0	a_2	0
3	θ_3	0	a_3	0
4	θ_4	0	a_4	-90

Table (3) Denavit-Hartenberg link parameters

From this table it is possible to formulate the homogeneous transformation matrix for each individual joint.

Joint (1)

$$R_0^1 = \begin{bmatrix} C_1 & -S_1 & 0 \\ S_1 & C_1 & 0 \\ 0 & 0 & 1 \end{bmatrix} \begin{bmatrix} 1 & 0 & 0 \\ 0 & 1 & 0 \\ 0 & 0 & 1 \end{bmatrix} = \begin{bmatrix} C_1 & 0 & S_1 \\ S_1 & 0 & -C_1 \\ 0 & 1 & 0 \end{bmatrix} \qquad d_0^1 = \begin{bmatrix} 0 \\ 0 \\ d_1 \end{bmatrix}$$

$$T_0^1 = \left[\begin{array}{ccc|c} C_1 & 0 & S_1 & 0 \\ S_1 & 0 & -C_1 & 0 \\ 0 & 1 & 0 & d_1 \\ \hline 0 & 0 & 0 & 1 \end{array}\right]$$

Joint (2)

$$T_1^2 = \left[\begin{array}{ccc|c} C_2 & -S_2 & 0 & a_2C_2 \\ S_2 & C_2 & 0 & a_2S_2 \\ 0 & 0 & 1 & 0 \\ \hline 0 & 0 & 0 & 1 \end{array}\right]$$

Joint (3)

$$T_2^3 = \left[\begin{array}{ccc|c} C_3 & -S_3 & 0 & a_3C_3 \\ S_3 & C_3 & 0 & a_3S_3 \\ 0 & 0 & 1 & 0 \\ \hline 0 & 0 & 0 & 1 \end{array}\right]$$

Joint (4)

$$R_3^4 = \begin{bmatrix} C_4 & -S_4 & 0 \\ S_4 & C_4 & 0 \\ 0 & 0 & 1 \end{bmatrix}\begin{bmatrix} 1 & 0 & 0 \\ 0 & 0 & 1 \\ 0 & -1 & 0 \end{bmatrix} = \begin{bmatrix} C_4 & 0 & -S_4 \\ S_4 & 0 & C_4 \\ 0 & -1 & 0 \end{bmatrix} \qquad d_3^4 = \begin{bmatrix} a_4C_4 \\ a_4S_4 \\ 0 \end{bmatrix}$$

$$T_3^4 = \left[\begin{array}{ccc|c} C_4 & 0 & -S_4 & a_4C_4 \\ S_4 & 0 & C_4 & a_4S_4 \\ 0 & -1 & 0 & 0 \\ \hline 0 & 0 & 0 & 1 \end{array}\right]$$

The overall homogeneous transformation matrix for the excavator arm is found using a chaining operation on the above matrices.

$$T_0^4 = T_0^1 T_1^2 T_2^3 T_3^4$$

$$T_0^4 = \left[\begin{array}{ccc|c} C_1 & 0 & S_1 & 0 \\ S_1 & 0 & -C_1 & 0 \\ 0 & 1 & 0 & d_1 \\ \hline 0 & 0 & 0 & 1 \end{array}\right]\left[\begin{array}{ccc|c} C_2 & -S_2 & 0 & a_2C_2 \\ S_2 & C_2 & 0 & a_2S_2 \\ 0 & 0 & 1 & 0 \\ \hline 0 & 0 & 0 & 1 \end{array}\right]\left[\begin{array}{ccc|c} C_3 & -S_3 & 0 & a_3C_3 \\ S_3 & C_3 & 0 & a_3S_3 \\ 0 & 0 & 1 & 0 \\ \hline 0 & 0 & 0 & 1 \end{array}\right]\left[\begin{array}{ccc|c} C_4 & 0 & -S_4 & a_4C_4 \\ S_4 & 0 & C_4 & a_4S_4 \\ 0 & -1 & 0 & 0 \\ \hline 0 & 0 & 0 & 1 \end{array}\right]$$

$$T_2^4 = \left[\begin{array}{ccc|c} C_3C_4 - S_3S_4 & 0 & -C_3S_4 - S_3C_4 & C_3a_4C_4 - S_3S_4a_4 + a_3C_3 \\ S_3C_4 + C_3S_4 & 0 & -S_4S_3 + C_3C_4 & S_3a_4C_4 + C_3S_4a_4 + a_3S_3 \\ 0 & -1 & 0 & 0 \\ \hline 0 & 0 & 0 & 1 \end{array}\right]$$

Using trigonometry identity the equation is reduced:

$$T_2^4 = \left[\begin{array}{ccc|c} Cos(\theta_3+\theta_4) & 0 & Sin(\theta_3+\theta_4) & a_4Cos(\theta_3+\theta_4)+a_3C_3 \\ Sin(\theta_3+\theta_4) & 0 & Cos(\theta_3+\theta_4) & a_4Sin(\theta_3+\theta_4)+a_3S_3 \\ 0 & -1 & 0 & 0 \\ \hline 0 & 0 & 0 & 1 \end{array}\right]$$

$$T_1^4 = \left[\begin{array}{ccc|c} C_2(Cos(\theta_3+\theta_4))-S_2(Sin(\theta_3+\theta_4)) & 0 & C_2(Sin(\theta_3+\theta_4))-S_2((Cos(\theta_3+\theta_4)) & \begin{array}{c} C_2(a_4Cos(\theta_3+\theta_4)+a_3C_3) \\ -S_2(a_4Sin(\theta_3+\theta_4)+a_3S_3) \\ +a_2C_2 \end{array} \\ S_2(Cos(\theta_3+\theta_4))+C_2(Sin(\theta_3+\theta_4)) & 0 & S_2(Sin(\theta_3+\theta_4))+C_2((Cos(\theta_3+\theta_4)) & \begin{array}{c} S_2(a_4Cos(\theta_3+\theta_4)+a_3C_3) \\ +C_2(a_4Sin(\theta_3+\theta_4)+a_3S_3) \\ +a_2S_2 \end{array} \\ 0 & -1 & 0 & 0 \\ \hline 0 & 0 & 0 & 1 \end{array}\right]$$

Again using trigonometry identity the equation is reduced

$$T_1^4 = \left[\begin{array}{ccc|c} Cos(\theta_2+\theta_3+\theta_4) & 0 & Sin(\theta_2+\theta_3+\theta_4) & a_4(Cos(\theta_2+\theta_3+\theta_4))+a_3(Cos(\theta_2+\theta_3))+a_2C_2 \\ Sin(\theta_2+\theta_3+\theta_4) & 0 & Cos(\theta_2+\theta_3+\theta_4) & a_4(Sin(\theta_2+\theta_3+\theta_4))+a_3(Sin(\theta_2+\theta_3))+a_2S_2 \\ 0 & -1 & 0 & 0 \\ \hline 0 & 0 & 0 & 1 \end{array}\right]$$

$$T_0^4 = \left[\begin{array}{ccc|c} C_1(Cos(\theta_2+\theta_3+\theta_4)) & -S_1 & C_1(Sin(\theta_2+\theta_3+\theta_4)) & C_1(a_4(Cos(\theta_2+\theta_3+\theta_4))+a_3(Cos(\theta_2+\theta_3))+a_2C_2) \\ S_1(Cos(\theta_2+\theta_3+\theta_4)) & C_1 & S_1(Sin(\theta_2+\theta_3+\theta_4)) & S_1(a_4(Sin(\theta_2+\theta_3+\theta_4))+a_3(Sin(\theta_2+\theta_3))+a_2S_2) \\ Sin(\theta_2+\theta_3+\theta_4) & 0 & Cos(\theta_2+\theta_3+\theta_4) & a_4(Sin(\theta_2+\theta_3+\theta_4))+a_3(Sin(\theta_2+\theta_3))+a_2S_2)+d_1 \\ \hline 0 & 0 & 0 & 1 \end{array}\right]$$

Using trigonometry identity and equating

1. $Cos(\theta_1+\theta_2+\theta_3+\theta_4) = C_{1234}$
2. $Sin(\theta_1+\theta_2+\theta_3+\theta_4) = S_{1234}$

The homogeneous transformation matrix equation is reduced and the arm matrix for the excavator is calculated as:

$$T_0^4 = \left[\begin{array}{ccc|c} C_1C_{234} & -S_1 & -C_1S_{234} & C_1(a_4C_{234}+a_3C_{23}+a_2C_2) \\ S_1C_{234} & C_1 & -S_1S_{234} & S_1(a_4C_{234}+a_3C_{23}+a_2C_2) \\ S_{234} & 0 & C_{234} & a_4S_{234}+a_3S_{23}+a_2S_2+d_1 \\ \hline 0 & 0 & 0 & 1 \end{array}\right]$$

From the homogeneous transformation matrix it can be seen that the vibro lance pivotal position and orientation is a function of the joint displacement.

$$\boxed{\theta_1\theta_2\theta_3\theta_4}$$

4.6 Inverse kinematic solution

The direct kinematic solution calculated in section (3.5) has provided the kinematic relationship between each of the excavator arm joints. The next step in the kinematic evaluation process, is to calculate the joint movement or rotation needed to position the vibro lance pivotal (joint 4) at a desired (x, y, z) co ordinate. The inverse kinematic solution is a process of equating the excavator arm matrix with the required arm position and orientation matrix. Once the relationship of each joint angle (θ) for a given (x, y, z) co ordinate is calculated, the movement needed to obtain a vertical motion will be obtained by rotating each individual arm joint to a determined angle (θ).

$$T_0^4 = \left[\begin{array}{ccc|c} C_1C_{234} & -S_1 & -C_1S_{234} & C_1(a_4C_{234}+a_3C_{23}+a_2C_2) \\ S_1C_{234} & C_1 & -S_1S_{234} & S_1(a_4C_{234}+a_3C_{23}+a_2C_2) \\ S_{234} & 0 & C_{234} & a_4S_{234}+a_3S_{23}+a_2S_2+d_1 \\ \hline 0 & 0 & 0 & 1 \end{array}\right] = \left[\begin{array}{ccc|c} R_{11} & R_{12} & R_{13} & X \\ R_{21} & R_{22} & R_{23} & Y \\ R_{31} & R_{32} & R_{33} & Z \\ \hline 0 & 0 & 0 & 1 \end{array}\right]$$

Joint (1)

$$\frac{\sin\theta_1}{\cos\theta_1} = \tan\theta_1 \therefore \tan\theta_1 = \frac{-R_{12}}{R_{22}}$$

$$\boxed{\theta_1 = \tan^{-1}\frac{-R_{12}}{R_{22}}}$$

Joint (3)

$$X = C_1(a_4C_{234} + a_3C_{23} + a_2C_2) \qquad (1)$$

$$Z = a_4S_{234} + a_3S_{23} + a_2S_2 + d_1 \qquad (2)$$

Equations (1 and 2) can be represented as two simultaneous equations. The solution is found by squaring and adding the equations.

Rearranging (1 and 2) gives:

$$a_3C_{23} + a_2C_2 = \frac{X}{C_1} - a_4C_{234} \qquad (3)$$

And

$$a_3S_{23} + a_2S_2 = Z - a_4S_{234} - d_1 \qquad (4)$$

Squaring the left side of equation (3)

$$(a_3C_{23} + a_2C_2)(a_3C_{23} + a_2C_2) = (a_3C_{23})^2 + a_3C_{23}a_2C_2 + a_3C_{23}a_2C_2 + (a_2C_2)^2$$
$$= (a_3C_{23})^2 + 2a_3C_{23}a_2C_2 + (a_2C_2)^2 \qquad (5)$$

Squaring the left side of equation (4)

$$(a_3S_{23} + a_2S_2)(a_3S_{23} + a_2S_2) = (a_3S_{23})^2 + a_3S_{23}a_2S_2 + a_3S_{23}a_2S_2 + (a_2S_2)^2$$
$$= (a_3S_{23})^2 + 2a_3S_{23}a_2S_2 + (a_2S_2)^2 \qquad (6)$$

Adding equations (5 and 6) grouping together similar quantities and using trigonometry identity produces:

$$a_2^2(C_2^2 + S_2^2) = a_2^2$$

$$a_3^2(C_{23}^2 + S_{23}^2) = a_3^2$$

$$2a_3S_{23}a_2S_2 + 2a_3C_{23}a_2C_2 = 2a_3a_2(C_{23}C_2 + S_{23}S_2) = 2a_3a_2C_3$$

Sub back into equation (3 and 4) and square the right hand side:

$$a_3^2 + a_2^2 + 2a_2a_3C_3 = \left(\frac{X}{C_1} - a_4C_{234}\right)^2 + (Z - a_4S_{234} - d_1)^2$$

Therefore

$$\theta_3 = \pm\cos^{-1}\left[\frac{\left(\frac{X}{C_1} - a_4C_{234}\right)^2 + (Z - a_4S_{234} - d_1)^2 - a_3^2 - a_2^2}{2a_2a_3}\right]$$

For joint (2)

$$x = C_1(a_4C_{234} + a_3C_{23} + a_2C_2) \qquad (1)$$

$$z = a_4S_{234} + a_3S_{23} + a_2S_2 + d_1 \qquad (2)$$

Re-arranging equations (1 and 2) by using trigonometry identity to find (S_2):

$$a_3C_2C_3 - a_3S_2S_3 + a_2C_2 = \frac{x}{C_1} - a_4C_{234}$$

$$S = C_2(a_3C_3 + a_2) - (a_3S_3)S_2 \qquad (3) \qquad \text{Where } S = \frac{x}{C_1} - a_4C_{234}$$

$$a_3S_2C_3 + a_3S_3C_2 + a_2S_2 = Z - d_1 - a_4S_{234}$$

$$T = S_2(a_2 + C_3a_3) + (a_3S_3)C_2 \qquad (4) \qquad \text{Where } T = Z - d_1 - a_4S_{234}$$

Equations (3 and 4) can be represented as two simultaneous equations.

$$(a_3S_3)S = C_2(a_3C_3 + a_2)(a_3S_3) - (a_3S_3)^2S_2 \qquad (5)$$

$$(a_3C_3 + a_2)T = (a_2 + C_3a_3)(a_3S_3)C_2 + S_2(a_2 + C_3a_3)^2 \qquad (6)$$

The solution is found by subtracting equations (5 and 6).

$$(a_3C_3 + a_2)T - (a_3S_3)S = S_2(a_2 + C_3a_3)^2 + (a_3S_3)^2 S_2 \quad (7)$$

Re-arrange equation (7) to find S_2 :

$$S_2 = \frac{(a_3C_3 + a_2)T - (a_3S_3)S}{(a_2 + C_3a_3)^2 + (a_3S_3)^2}$$

Equating (3 and 4) as two simultaneous equations.

$$(a_3C_3 + a_2)S = C_2(a_3C_3 + a_2)^2 - (a_3S_3)(a_3C_3 + a_2)S_2 \quad (8)$$

$$(a_3S_3)T = (a_3S_3)^2 C_2 + S_2(a_2 + C_3a_3)(a_3S_3) \quad (9)$$

Adding (8 and 9) gives:

$$(a_3C_3 + a_2)S + (a_3S_3)T = C_2(a_2 + C_3a_3)^2 + (a_3S_3)^2 C_2 \quad (10)$$

Re-arranging equations (10) to find (C_2):

$$C_2 = \frac{(a_3C_3 + a_2)S + (a_3S_3)T}{(a_2 + C_3a_3)^2 + (a_3S_3)^2}$$

$$\text{Therefore } \boxed{\theta_2 = \tan^{-1}\left[\frac{(a_3C_3 + a_2)T - (a_3S_3)S}{(a_2 + C_3a_3)S + (a_3S_3)T}\right]}$$

From the rule that states the previous homogeneous transformation matrix must equal the new transformation matrix with required position and orientation:

$$\frac{S_{234}}{C_{234}} = \frac{R_{31}}{R_{33}}$$

$$\tan\theta_4 = \frac{R_{31}}{R_{33}} - \theta_2 - \theta_3 \qquad \therefore \qquad \boxed{\theta_4 = \tan^{-1}\frac{R_{31}}{R_{33}} - \theta_2 - \theta_3}$$

4.7 Joints (2, 3) kinematics solutions.

The objective of the vibro verticality controller is to manipulate in a vertical manner the vibro lance as shown in figure (12). The relative angle between the upper carriage and the tracks is irrelevant to the design of the controller, therefore $(\theta_1 = 0)$.

It is assumed that +ve (X) motion for the arm is away from the machine and –ve motion is towards. The same goes for +ve (Z) which is arm up and –ve (Z) arm down. As for the joints, clockwise motion indicates +ve movement whereas –ve motion indicates anticlockwise movement. From these rules the inverse kinematic solutions for joints (2, 3) are reduced to:

$$\theta_3 = \cos^{-1}\left[\frac{(X)^2 + (Z - d_1)^2 - (a_3^2 + a_2^2)}{2a_2a_3}\right]$$

θ_1 *and* θ_2 Solutions are modified to ensure joint up scenario

$$\theta_2 = \tan^{-1}\left[\frac{(a_3C_3 + a_2)(Z - d_1) - (a_3S_3)X}{(a_2 + C_3a_3)X - (a_3S_3)(Z - d_1)}\right]$$

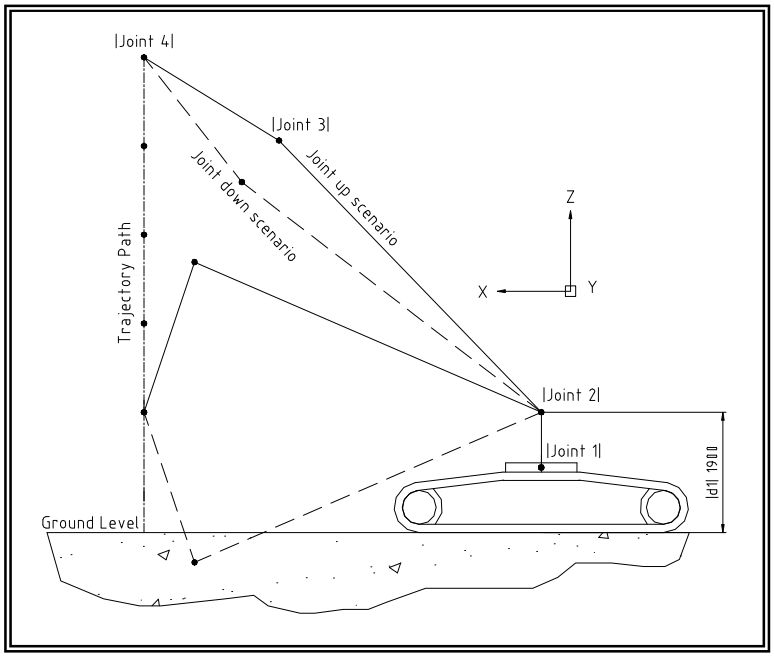

Figure (29) represents the joint up / joint down

With the inverse kinematic solution completed for each joint, it's clear to see that all of the revolute joints have a unique solution except joint (3). Here the joint may have a +ve value (joint up) or a –ve value (joint down) angle to orientate and position the vibro lance pivotal at the desired x, y and z co ordinate. Due to the limitation of the excavator arm joints, the up solution is the only choice. See figure (13) for a schematic representation of the joint up / joint down scenario.

5.0 Trajectory planning

Trajectory planning is a method of assigning a path for the four joints of the excavator arm to follow. The path is designed to move the vibro pivotal from its starting (x, y, z) co ordinates to the desired vertical position and orientation, keeping within the excavator arm capabilities. Along with the path assignment a time profile for each joint will be calculated. The pivotal trajectory can be planned either in joint space (directly specifying the time evolution of the joint angle) or in Cartesian space (specifying the position and orientation of the end frame).

5.1 Joint Space trajectories [7]

With the simplest case having a starting joint position q_0 an end joint position q_1 over a set time interval $(t_0) \Rightarrow (t_f)$, it is possible to use cubic polynomials with 4 coefficients. They can be used to satisfy both position and velocity constraints at the initial and final position.

For the excavator arm joint variables, the constraints are:

$q_i(t_0) = q_0$	$q_i(t_f) = q_1$
$\dot{q}_i(t_0) = \dot{q}_0$	$\dot{q}_i(t_f) = \dot{q}_1$

Where:

(t_0) = Start time
(t_f) = End time
$(q_0) \& \left(\dot{q}_0\right)$ = The initial position and velocity
$(q_1) \& \left(\dot{q}_1\right)$ = The final position and velocity

The cubic polynomial for joint position and its derivative for joint velocity are:

$$q_i(t) = a_0 + a_1 t + a_2 t^2 + a_3 t^3 \quad \ldots 1$$
$$\dot{q}_i(t) = a_1 + 2a_2 t + 3a_3 t^2 \quad \ldots 2$$

At the initial condition when $(t_0) = 0$ then:

$$q_i(0) = a_0 = q_0 \quad \ldots 3$$
$$\dot{q}_i(0) = a_1 = \dot{q}_0 \quad \ldots 4$$

It is now possible to find (a_2 & a_3) from the final conditions by substituting (a_0 & a_1) into equation (5 & 6)

$$q_i(t_f) = q_0 + \dot{q}_0 t_f + a_2 t_f^2 + a_3 t_f^3 = q_1 \qquad \ldots 5$$

$$\dot{q}_i(t_f) = \dot{q}_0 + 2a_2 t_f + 3a_3 t_f^2 = \dot{q}_1 \qquad \ldots 6$$

Equations (5 & 6) can be treated as a pair of simultaneous equations. Therefore to find a_2 eliminate a_3 by multiplying equation (5) by (3) and subtract the equations from one another.

$$3q_1 = 3q_0 + 3\dot{q}_0 t_f + 3a_2 t_f^2 + 3a_3 t_f^3 \qquad \ldots 7$$

Multiplying equation (6) by (t_f) gives:

$$\dot{q}_1(t_f) = \dot{q}_0 t_f + 2a_2 t_f^2 + 3a_3 t_f^3 \qquad \ldots 8$$

Subtract equation (8 from 7) gives:

$$3q_1 - \dot{q}_1(t_f) = 3q_0 + 3\dot{q}_0 t_f + 3a_2 t_f^2 + 3a_3 t_f^3 - \dot{q}_0 t_f - 2a_2 t_f^2 - 3a_3 t_f^3$$

Hence:

$$a_2 = \left(\frac{3(q_1 - q_0) - \left(2\dot{q}_0 + \dot{q}_1\right) t_f}{t_f^2} \right)$$

Similar to find a_3 eliminate a_2 by multiplying equation 5 by (2) and subtract the equation from each other gives:

$$a_3 = \left(\frac{2(q_0 - q_1) - \left(\dot{q}_0 + \dot{q}_1\right) t_f}{t_f^3} \right)$$

To simplify the controller it would be favourable to generate the trajectory in joint space and use this method of interpolating the joints from one position to another. As the actual control of the excavator arm in this case occurs in joint space there is no need to invoke the use of inverse kinematics which in-turn reduces the computation time of the controller. Disadvantage using this method of control is that the actual position of the vibro pivotal will sometimes be unclear. The main feature that the controller must have is the ability to drive the vibro lance in a vertical manner into the ground. Any large deviation from the vertical will hail the vertical controller useless. See figure (30) for a possible scenario of the excavator arm trajectory using the joint space method.

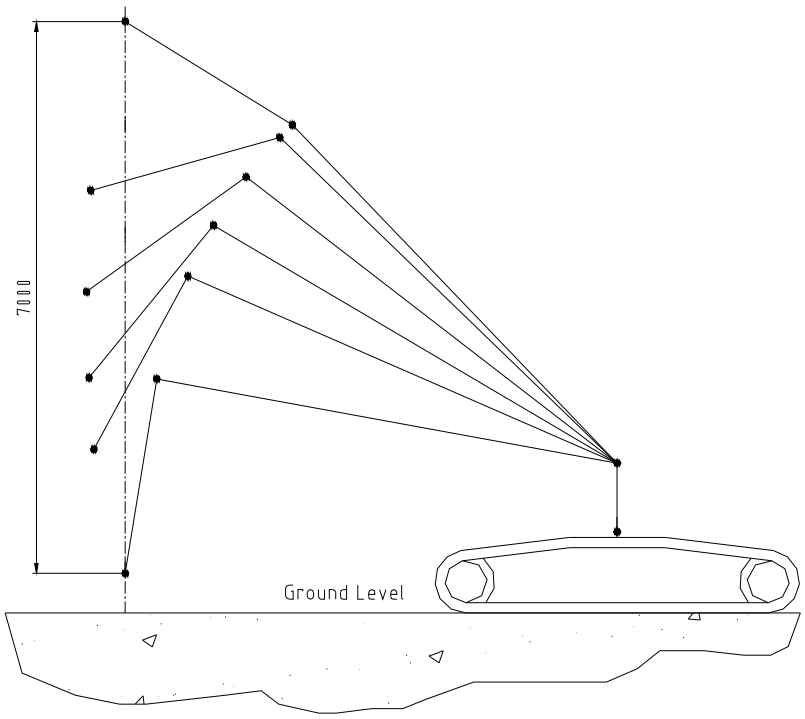

Figure (30) possible trajectory scenario using the joint space control method

However, as this is only a trajectory possibility at this stage in the vertical controller design, we may find that a simple linear interpolation in joint space is good enough for the excavator arm controller.

5.2 Cartesian space straight line trajectory

Here the (x, y, z) co ordinates for the vibro pivotal start and end location are calculated. To ensure the verticality of the vibro lance the vertical trajectory is divided up into a number of equally spaced points (N). The inverse kinematics on each of these (N) interval points is calculated. The excavator arm joints will pass through the inverse kinematics joint solutions ensuring a straight line trajectory of the vibro pivotal. To keep the computational time down to minimum for the controller an estimated interval point number of (5) will be used at this stage in the design. It may be found later that this interval trajectory point (N) can be reduced or needs to be increased so as not to deviate from the straight line path.

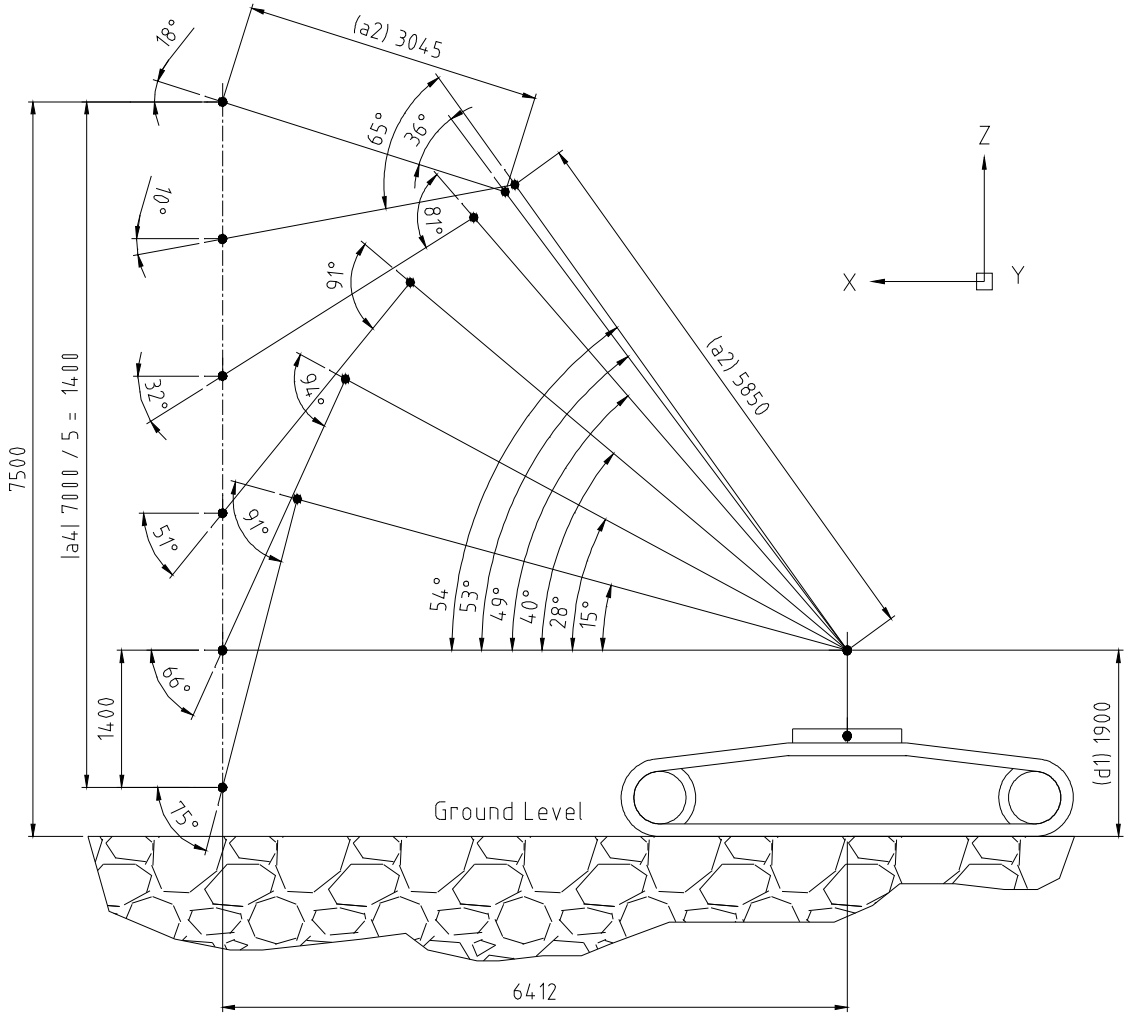

Figure (31) Cartesian space straight line trajectory with (5) interval points

5.3 Excavator arm trajectory and path planning

Section (4.6) has provided solutions for joint angles to position the excavator arm at specified (x, y and z) coordinates. The controller design will provide a continuous vertical path motion for the vibro pivotal. The straight line motion can be modelled for the three phases of motion as:

1. Initial ramping up speed from (X_0, Y_0, Z_0)
2. Constant velocity (straight line trajectory)
3. Final ramping down speed to (X_f, Y_f, Z_f)

Where the initial (X_0, Y_0, Z_0) are the excavator arm start coordinates and (X_f, Y_f, Z_f) are the final excavator arm coordinates.

As shown in section (4.6) $[T_0^4(0)]$ *and* $[T_0^4(T)]$ denotes the "start point" and "end point" of the excavator arm respectively. If the overall trajectory movement is to be carried out in (T) seconds, then the general straight line trajectory for the vibro pivot can be represented as:

$$[T_0^4(t)] = [1 - S(t)][T_0^4(0)] + S(t)[T_0^4(T)]$$

$S(t)$ Is the % of the overall distance travelled, with $S(0) = 0$ and $S(T) = 1$ for the initial and end conditions. The trajectory motion of the excavator arm will start its movement with constant acceleration until it reaches its running speed. It will then continue at constant velocity along a mapped out path, until final slowing down at a constant velocity to reach its end position. For the instants of straight line motion with equal ramping up and down, the speed distribution function is shown in figure (32).

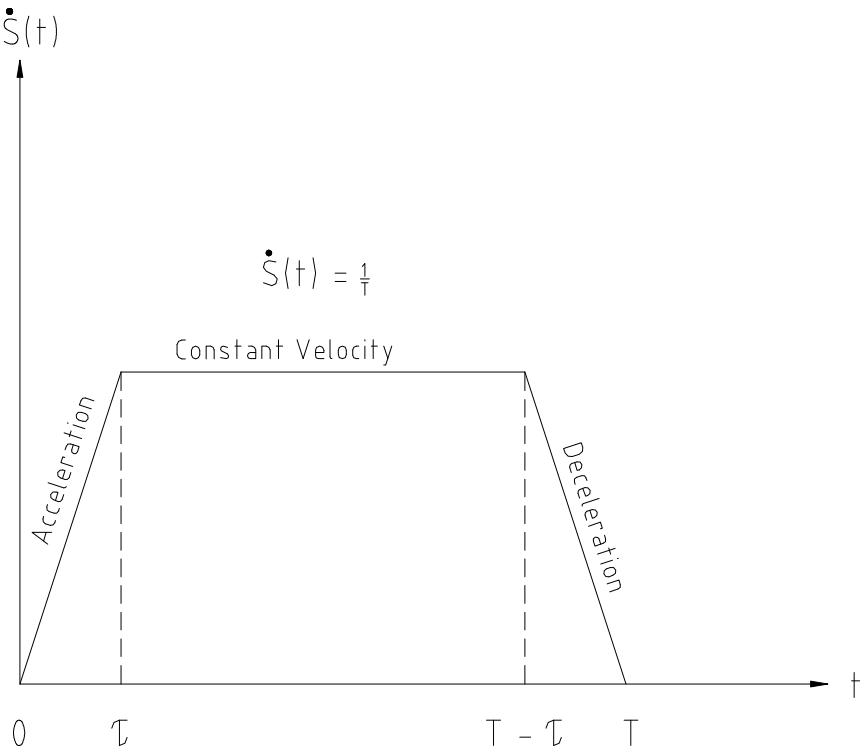

Figure (32) typical speed profile curve

The acceleration and deceleration values for the excavator arm joints will depend upon the value of τ . Therefore an expression for the speed profile outlined above in figure (15) within the range (0, τ) would be:

$$\dot{S}(t) = K_1 t \qquad (1)$$

Where K_1 is found using the general equation for a straight line in the form $y = mx + c \;\; \therefore K_1 = \frac{1}{\tau T}$ (2)

Sub back in (1)

$$\dot{S}(t) = \frac{t}{\tau T} \qquad \therefore S(t) = \frac{t^2}{2\tau T} + K_2 \qquad (3)$$

At the initial condition $(T=0) and (t=0)$ then $K_2 = 0$

Equation (3) can be re-written as $S(t) = \frac{t^2}{2\tau T}$ when $0 \le t \le \tau$

At constant velocity within the range $\tau \le t \le (T-\tau)$ then $\dot{S}(t) = \frac{1}{T}$ (4) $\therefore S(t) = \frac{t}{T}$

Finally in the deceleration phase of the excavator arm trajectory when $(T-\tau) \le t \le T$ and assuming the speed profile follows a linear form then:

$$\dot{S}(t) = K_3 t + K_4 \qquad (5)$$

Within this phase of the trajectory the initial conditions are at $t = (T-\tau)$ when $\dot{S}(t) = \frac{1}{T}$ and at $t = T$ when $\dot{S}(t) = 0$

Therefore equation (5) is solved using a simultaneous equation with two unknowns.

$$\frac{1}{T} = K_3(T-\tau) + K_4 \qquad (6)$$

$$0 = K_3(T) + K_4 \qquad (7)$$

Subtract (7) from (6) gives:

$$\frac{1}{T} = K_3[(T-\tau) - T] \therefore K_3 = \frac{-1}{T\tau} \qquad (8)$$

Sub (8) back into (7) gives:

$$K_4 = \frac{1}{\tau}$$

Equation (5) is now re-written as:

$$\dot{S} = \frac{1}{\tau} - \frac{t}{\tau T} \qquad (9) \therefore S(t) = \frac{t}{\tau} - \frac{t^2}{2\tau T} + K_5 \qquad (10)$$

At the final condition $(t = T) and\ S(t) = 1$ then $K_5 = 1 - \frac{T}{2\tau}$

Sub back into (10) gives:

$$S(t) = 1 - \frac{T}{2\tau} + \frac{t}{\tau} - \frac{t^2}{2\tau T}$$

From the above it can now be concluded that:

$S(t)$ Is the % of the overall distance travelled with $S(0) = 0 and\ S(T) = 1$

Where

$T =$	The overall time period for the excavator arm motion
$t =$	Instantaneous time
$[T_0^4(0)] =$	The initial arm position
$[T_0^4(T)] =$	The final arm position

$$S(t) = \frac{t^2}{2\tau T} \qquad \text{When} \quad 0 \le t \le \tau$$

$$S(t) = \frac{t}{T} \qquad \text{When} \quad \tau \le t \le (T - \tau)$$

$$S(t) = 1 - \frac{T}{2\tau} + \frac{t}{\tau} - \frac{t^2}{2\tau T} \qquad \text{When} \quad (T - \tau) \le t \le T$$

$$[T_0^4(t)] = [1 - S(t)][T_0^4(0)] + S(t)[T_0^4(T)] \qquad \text{When} \quad 0 \le t \le T$$

At this stage in the project it is assumed that the excavator arm will move the vibro pivotal from an initial position of $[6.412, \quad 7.5, \quad 0]$ to an end position of $[6.412, \quad -1.4, \quad 0]$ in a time period $T = 60s$. Although the initial speed ramping up and down phases of the hydraulic rams that manipulate the excavator arm will be milliseconds, for the schematic representation of the speed profile, the acceleration and deceleration periods will be $0.033 \times T$. From these assumptions the speed profile will take the form outlined in figure (33) and the boom and arm joint angles represented by figure (34) with respect to $S(t)$. The vibro pivotal position with respect with time (t) is calculated from:

$$[T_0^4(t)] = \begin{bmatrix} X(0)[1 - S(t)] + X(T)S(t) \\ Y(0)[1 - S(t)] + Y(T)S(t) \\ 0 \end{bmatrix}$$

Figure (33)
Vibro pivitol speed profile
Overall trajectoty time period = (60s)
Acceleration/Decelaration phase = (2s)

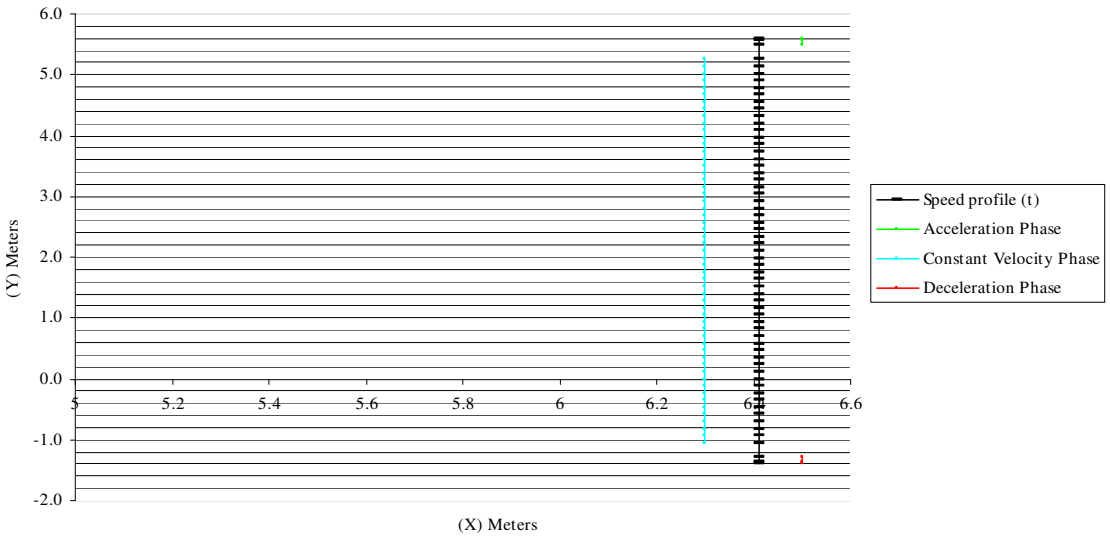

Figure (34)
Excavator joint Angle relative to time (t)
(X0, Y0 = 6.412, 7.5) (Xf, Yf = 6.412, -1.4)

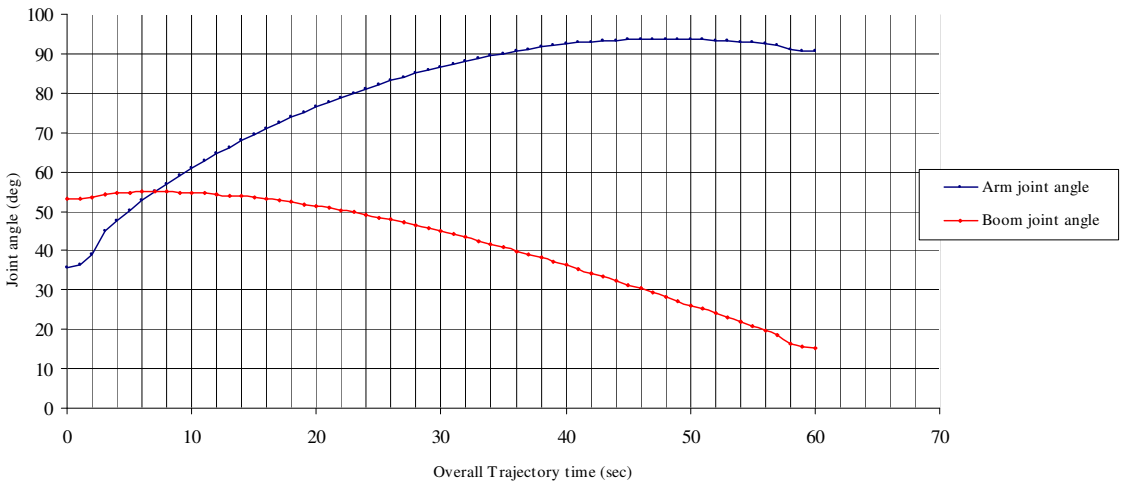

6.0 Control models and systems

6.1 Types of model [8]

There are many types of system and model design a few are described below:

- ***Lumped parameters:*** The inputs and outputs of the system are represented by a transfer function equation.

- ***Discrete time using the difference equation:*** The equation describes how the inputs and outputs of the system change with time.

- ***Non linear models:*** Hydraulic actuators, in combination with servo valves, are used to drive the arms of the excavator to position the vibro lance. The fluid flow within the hydraulic actuator inherently leads to nonlinear behaviour for the system. A control strategy is developed which is based upon the nonlinear model.

- ***Stochastic modelling:*** Mathematical models can be categorized broadly as being probabilistic or deterministic. There are Situations where probabilistic models are more suitable than the latter. Sometimes it is better to representation a system by considering a collection of random variables instead of a single one. Collections of random variables indexed by a parameter such as time are known as stochastic processes.

- ***Black box:*** In a black box software design, the user only knows the inputs and what the expected outcomes should be, not how the software arrives at those outputs. E.g. a transfer function obtained from a data-based analysis.

6.2 Types of controller

There are basically two types of controller see fig (35);

1. Open loop controller
2. Closed loop controller

Open loop controller: This type of control system design is simply power in, power out, there is no measurement or feedback from the output (y_k) and therefore the output of the system has no effect on the input or desired output (y_{dk}).

Closed loop controller: In contrast to the open loop control design the closed loop design has feedback from the output (y_{dk}) to control or influence the input signal (u_k). As will be seen later the automated verticality controller will be of the closed loop control design.

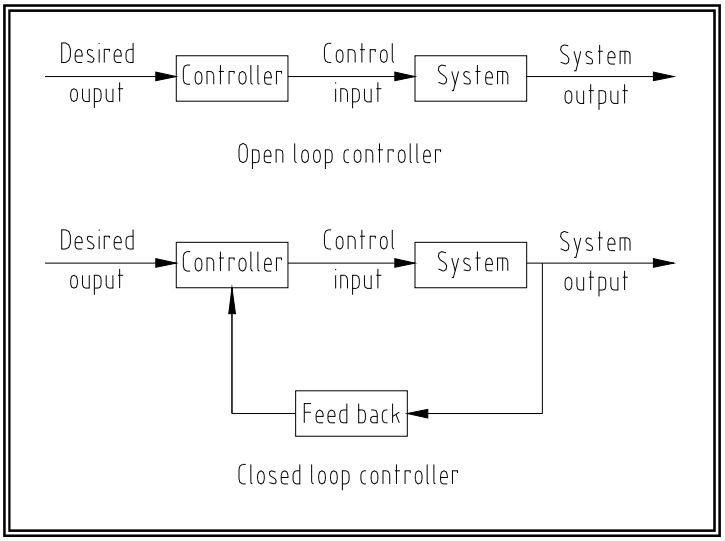

Figure (35) open and closed loop controllers

There are many approaches for modelling and controlling of a system, this report will outline the main types of control system but will concentrate primarily on the methods employed using state space methods for the modelling and (PIP) proportional integral plus for the controlling of the system.

6.3 Brief outline of the classical controller

The three main closed loop control structures are;

1. Proportional control
2. Integral control
3. Derivative control

Proportional control: Here the system error (e_t) is simply multiplied by a gain factor (K_p). This type of system design invokes a stead state error between the desired input and the measured output; the controller output never reaches the desired level.

Integral control: Although the control system is relatively slow to response to an input it does not suffer from a steady state error like with the proportional controller. The system error (e_t) is multiplied by an integrated $\left(K_I \int \right)$ to give a stead state system output.

Derivative control: The derivate controller is normally only used in conjunction with one or both of the other two controllers discussed. The derivative output value $\left(K_d \frac{d}{dt}\right)$ is based on the rate of change of the error signal (e_t). See figure (17) for a schematic representation of the three controllers where (u_k) and (y_k) are the controllers input and output respectively.

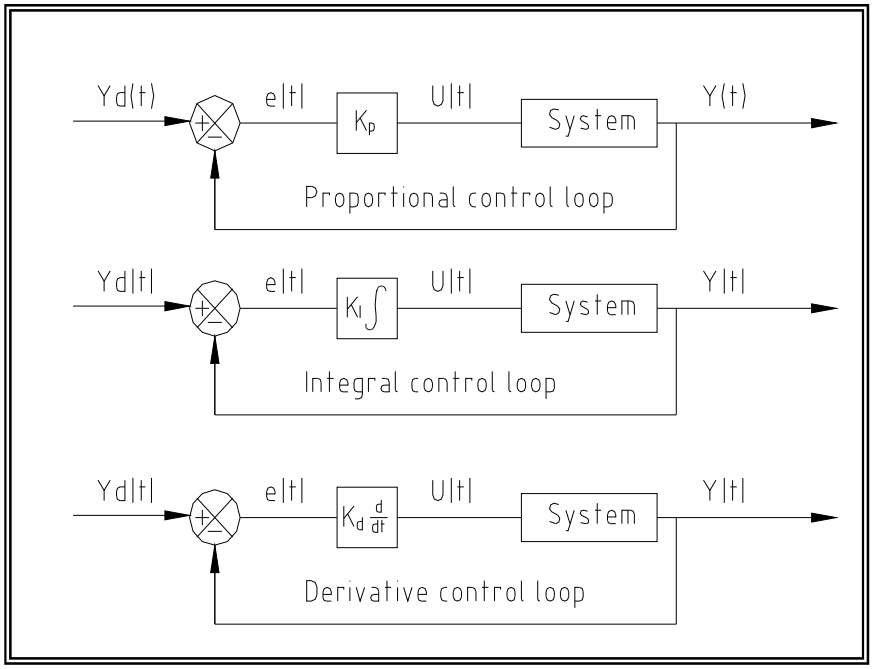

Figure (36) classical controller

If the system to be controlled is of first order then adequate control can be obtained using a combination of ***Proportional + Integral*** (PI) control. Whereas, if the system is capable of tolerating a stead state error between the input and output then ***Proportional + Derivate*** (PD) control can be used. When the control system is of second or higher order and good control of the system is required in the transient state then ***Proportional + Integral + plus*** (PIP) control systems are implemented.

The objective of the vibro controller is outlined as:

1. The closed loop system must be stable
2. The output signal must track the input signal at steady state
3. The controller output signal should have little overshoot or oscillation
4. The controller will reject undesired input or output disturbances

The design of the vibro controller system will be carried out in four stages:

1. System identification using advanced system identification techniques. (Developed at Lancaster university)
2. The design of a proportional-integral-plus (PIP) digital controller. (Lancaster university)
3. Evaluation of the design using computer simulation (Matlab)
4. The implementation of the controller onto the excavator (Komatsu)

6.4 The Non-minimal state space (NMSS) representation [8]

The discrete time transfer function model of a system can be represented as;

$$y(k) = \frac{b_1 z^{-1} + \ldots + b_m z^{-m}}{1 + a_1 z^{-1} + \ldots + a_n z^{-n}} u(k) \qquad (1)$$

Where $y(k)$ and $u(k)$ denote the sample output and input respectively, the NMSS model is defined as;

$$x(k) = Fx(k-1) + gu(k-1) + dy_d(k)$$
$$y(k) = hx(k)$$

The state vector $x(k)$ consists of the past and present sampled values of the output variable $y(k)$ the pasted input samples of $u(k)$ and there is also an integral of error state $z(k)$ introduced into the equation to ensure steady state tracking of the input. The value of $z(k)$ is the difference between the desired output and sampled output $y_d(k)$ and $y(k)$ respectively.

$$z(k) = z(k-1) + \{y_d(k) - y(k)\} \qquad (2)$$

Therefore the state matrix is defined as follows;

$$x(k) = [y(k) \quad y(k-1) \quad \ldots \quad y(k-n+1) \quad u(k-1) \quad u(k-2) \quad \ldots \quad u(k-m+1) \quad z(k)]^T$$

The state matrix can be seen in figure (37)

$$F = \begin{bmatrix} -a_1 & -a_2 & \cdots & -a_{n-1} & -a_n & b_2 & b_3 & \cdots & b_{m-1} & b_m & 0 \\ 1 & 0 & \cdots & 0 & 0 & 0 & 0 & \cdots & 0 & 0 & 0 \\ 0 & 1 & \cdots & 0 & 0 & 0 & 0 & \cdots & 0 & 0 & 0 \\ \vdots & \vdots & \ddots & \vdots & \vdots & \vdots & \vdots & \ddots & \vdots & \vdots & \vdots \\ 0 & 0 & \cdots & 1 & 0 & 0 & 0 & \cdots & 0 & 0 & 0 \\ 0 & 0 & \cdots & 0 & 0 & 0 & 0 & \cdots & 0 & 0 & 0 \\ 0 & 0 & \cdots & 0 & 0 & 1 & 0 & \cdots & 0 & 0 & 0 \\ 0 & 0 & \cdots & 0 & 0 & 0 & 1 & \cdots & 0 & 0 & 0 \\ \vdots & \vdots & \ddots & \vdots & \vdots & \vdots & \vdots & \ddots & \vdots & \vdots & \vdots \\ 0 & 0 & \cdots & 0 & 0 & 0 & 0 & \cdots & 1 & 0 & 0 \\ a_1 & a_2 & \cdots & a_{n-1} & a_n & -b_2 & -b_3 & \cdots & -b_{m-1} & -b_m & 1 \end{bmatrix}$$

$$g = \begin{bmatrix} b_1 & 0 & 0 & \cdots & 0 & 1 & 0 & 0 & \cdots & 0 & -b_1 \end{bmatrix}^T$$

$$d = \begin{bmatrix} 0 & 0 & 0 & \cdots & 0 & 0 & 0 & 0 & \cdots & 0 & 1 \end{bmatrix}^T$$

$$h = \begin{bmatrix} 1 & 0 & \cdots & 0 & 0 & 0 & 0 & \cdots & 0 & 0 & 0 \end{bmatrix}$$

Figure (37) state transition matrix

Where:

F = The state transition matrix

g = Is the input vector

d = Desired output vector

h = The output vector

For the excavator arm transfer function (TF) identification, the input-output data sent-received from the hydraulic control valves and excavator joint position will be collected and recorded on line. This will be achieved by manoeuvring the excavator arm via voltage signals sent to the hydraulic control valves that control the motion of the excavator arm. The past and present sampled values of the arm joint position $y(k)$ and the pasted input control voltages $u(k)$ can then be collected and stored in the state matrix form. Once the information has been gathered and stored the identification and estimation of the (TF) will be done using the methods available in the MATLAB© identification toolbox.

6.5 Overview of the PIP controller [9 10 11]

The PIP controller design (Young et al., 1987; Chotai et al., 1998., Taylor et al., 2000) has additional feedback which in-turn generates additional inputs; this allows for pole assignment in systems with either second order or higher (TF) transfer functions, or pure inherent time delays greater than one sample interval.

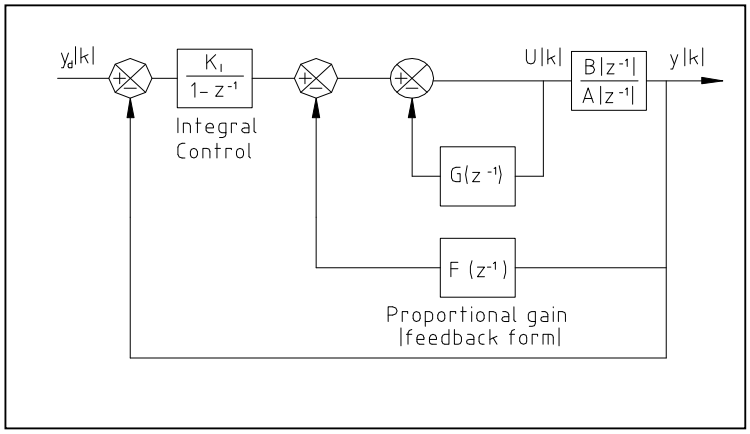

Where:

$$G(z^{-1}) = 1 + g_1 z^{-1} + \ldots + g_{m-1} z^{-m+1}$$
$$F(z^{-1}) = f_0 + f_1 z^{-1} + \ldots + f_{n-1} z^{-n+1}$$
$$A(z^{-1}) = 1 + a_1 z^{-1} + \ldots + a_{n-1} z^{-n}$$
$$B(z^{-1}) = b_1 z^{-1} + b_2 z^{-2} \ldots + b_m z^{-m}$$

Figure (38) PIP proportion Integral controller

The closed loop transfer function (TF) of the PIP controller shown in figure (19) is thus;

$$y(k) = \frac{k_1 B(z^{-1})}{(1-z^{-1})\left(G(z^{-1})A(z^{-1}) + F(z^{-1})B(z^{-1})\right) + K_I B(z^{-1})} y_d(k) \qquad (3)$$

As the desired input $y_d(k)$ reaches a constant value, the output $y(k)$ will reach and equilibrium level when $y(k) = y(k-1)$. Therefore $y(k)$ is found by setting $z^{-1} = 1$.

Doing this allows the PIP closed loop transfer function (TF) to be reduced to;

$$y(k) = \frac{k_1 B(z^{-1})}{K_I B(z^{-1})} y_d(k)$$ Showing that at steady state $y(k) = y_d(k)$

The PIP controller shown in figure (38) is basically an extension of the traditional PI (feedback) controller.

6.6 Designing the PIP controller

The design and implementation of the PIP controller was done using the Captain toolbox within the Matlab software environment. The Captain toolbox is capable of choosing a model that best suits the sampled data.

6.7 Collecting the data

When using the NMSS design method for the identification of the system, the transfer function (TF) is obtained from a measure of the input and output data of the system. The controller output signal to drive the excavator arm and boom joints ranged from ±1000, joint up positive and joint down negative movement. To ensure accurate modelling of the excavator joints for the full speed range, models of the system were done for every 100 speed intervals and there average (b, RT² and YIC) logged. See figure (39, 40 and 41) for the recorded values.

	Boom				Dipper		
Speed	(b)	Rt^2	YIC	Speed	(b)	Rt^2	YIC
-100	0.00063	0.9969	-18.982	-100	0.0013	0.9860	-15.8269
-200	0.0012	0.9965	-17.723	-200	0.0016	0.9965	-17.9642
-300	0.0017	0.9949	-16.4232	-300	0.0019	0.9972	-17.8398
-400	0.0022	0.995	-15.7763	-400	0.0028	0.9982	-17.8674
-500	0.0026	0.9952	-15.6428	-500	0.0034	0.9982	-17.4155
-600	0.0025	0.9976	-16.5926	-600	0.0045	0.9955	-15.1115
-700	0.0027	0.9976	-16.4449	-700	0.0051	0.9987	-17.2692
-800	0.0027	0.9979	-16.4931	-800	0.0046	0.9966	-15.3368
-900	0.0028	0.9971	-15.7775	-900	0.0043	0.9918	-13.3855
-1000	0.0031	0.9974	-15.7215	-1000	0.0049	0.9870	-12.3465
AVG	0.0022	0.9966	-16.5577	AVG	0.0034	0.9946	-16.0363
100	0.00091	0.9765	-14.0843	100	0.0052	0.9902	-14.6719
200	0.00071	0.9901	-15.8873	200	0.0061	0.9972	-16.6389
300	0.00071	0.9918	-16.1192	300	0.0072	0.9964	-15.5892
400	0.00077	0.9898	-15.3968	400	0.0083	0.9975	-15.3711
500	0.00080	0.9926	-15.4524	500	0.0094	0.9977	-15.6237
600	0.00086	0.9921	-15.2422	600	0.0090	0.9990	-17.2513
700	0.00096	0.9937	-15.4641	700	0.0083	0.9991	-17.6073
800	0.00091	0.9923	-14.8808	800	0.0072	0.9992	-17.4128
900	0.00098	0.9942	-15.3472	900	0.0066	0.9993	-17.2892
1000	0.001	0.9916	-14.4179	1000	0.0058	0.9983	-16.1739
AVG	0.0009	0.9905	-15.2292	AVG	0.0073	0.9974	-16.3629
Overall AVG	0.0015	0.9935	-15.8935	Overall AVG	0.0054	0.9960	-16.1996

Figure (39) is a log of the recorded (b) and model fits (RT² and YIC)

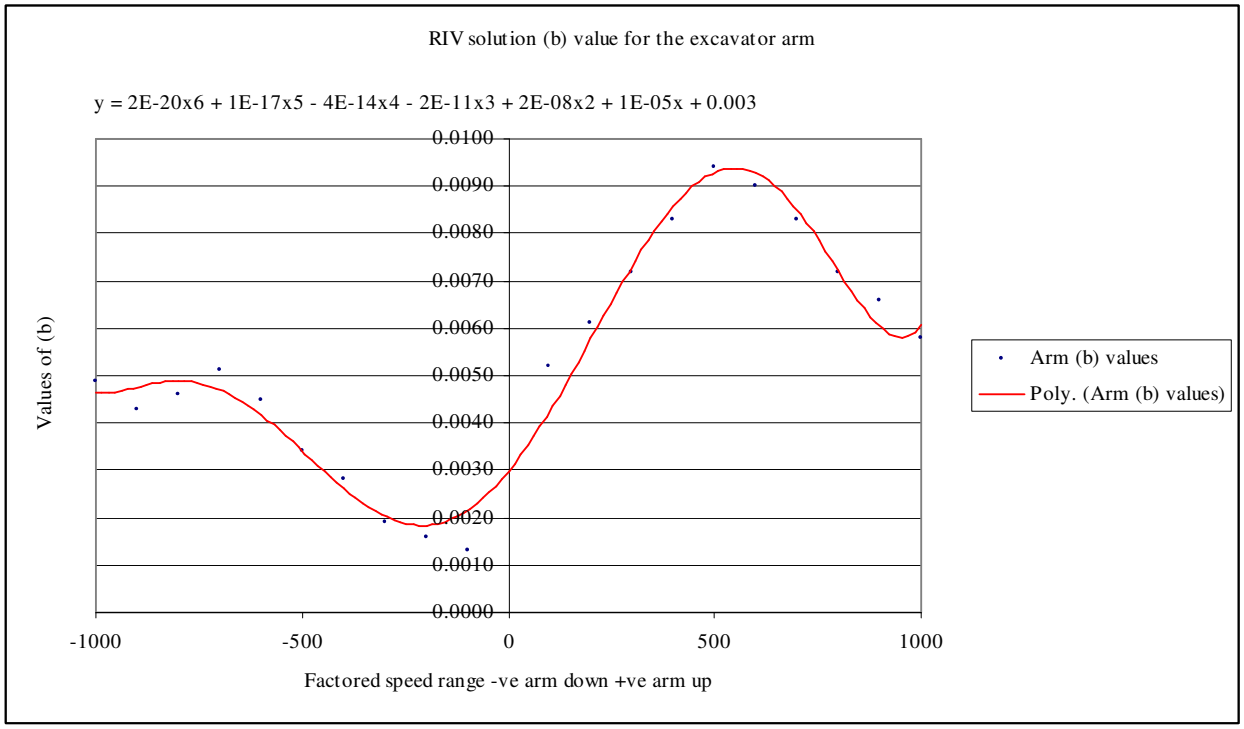

Figure (40) Calculated (b) value for the arm using RIV function

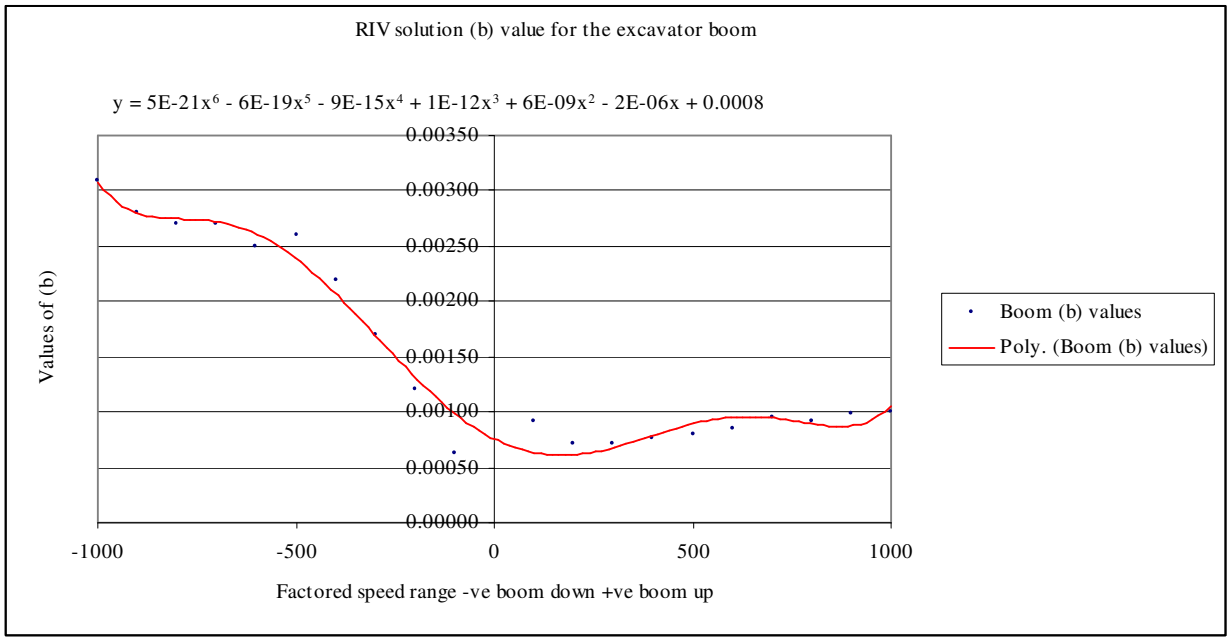

Figure (41) Calculated (b) value for the boom using RIV function

The identification of the model was obtained using the RIVID and RIV (Young, 1984, 1991) functions found inside Captains toolbox. See appendix for the Matlab program used to extract the best model parameters for each recorded speed. Using the tradition methods of trial and error appropriate system variable were inputted into the Matlab program, the system chooses models base on the RT^2 and YIC model results. The RT^2 method is based on the coefficient of determination, the closer the fit to unity the better the model fit. Whereas YIC is an indication as to how complicated the (TF) will be, the more negative the value of YIC the less parameters the model will have. The overall model chosen is thus a compromise between model fit and parameters. A typical boom and arm model fit using RIVID and RIV model function are pictures in figure (40 and 41) below.

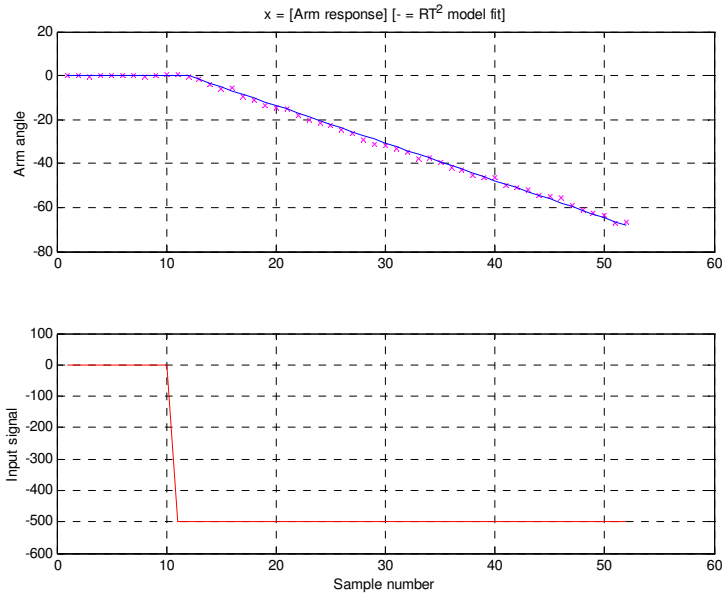

Figure (42) Arm response and model fit

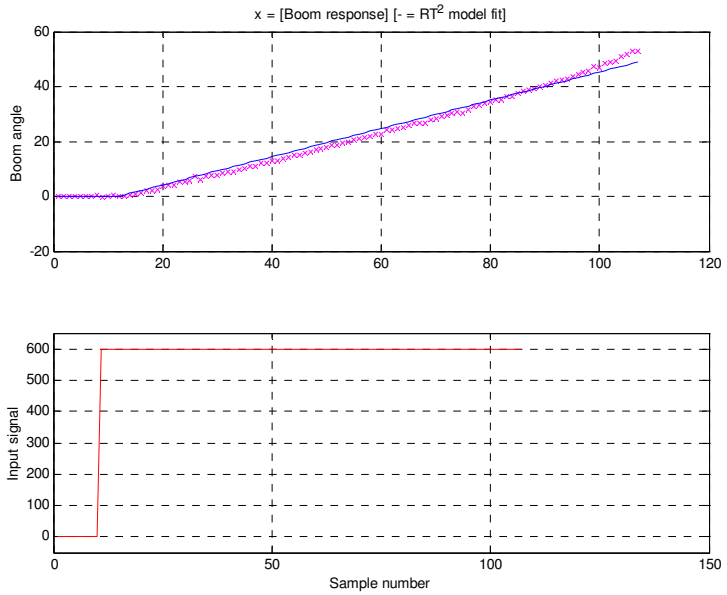

Figure (43) Boom response and model fit

6.8 Identifying the (SVF) from the RIV model

The RIV function estimated (TF) models for both joints of the excavator arm to be first order with two time delays therefore reducing equation (1):

$$y(k) = \frac{b_1 z^{-2}}{1 - a_1 z^{-1}} u(k) \text{ With a difference equation of } y(k) = -a_1 y_{(k-1)} + b_2 u_{(k-2)} \quad (4)$$

Substituting equation (4) into the integral of error equation (2) gives:

$$z(k) = z(k-1) + \{y_d(k) + a_1 y_{(k-1)} - b_2 u_{(k-2)}\}$$

The NMSS representation shown in figure (36) is reduced to for the modelling of the excavator arm (TF) see figure (37).

$$x(k) = \begin{bmatrix} y_k \\ u_{(k-1)} \\ z_k \end{bmatrix} = \begin{bmatrix} -a_1 & b_2 & 0 \\ 0 & 0 & 0 \\ a_1 & -b_1 & 1 \end{bmatrix} \begin{bmatrix} y_{(k-1)} \\ u_{(k-1)} \\ z_k \end{bmatrix} + \begin{bmatrix} 0 \\ 1 \\ 0 \end{bmatrix} u_{(k-1)} + \begin{bmatrix} 0 \\ 0 \\ 1 \end{bmatrix} y_{dk}$$

$$y(k) = \begin{bmatrix} 1 & 0 & 0 \end{bmatrix} \begin{bmatrix} y_k \\ u_{(k-1)} \\ z_k \end{bmatrix}$$

Figure (44) NMSS representation of the excavator arm

The state variable feedback (SVF) control law is defined as:

$$u(k) = -kx(k)$$

$$\therefore u(k) = -\begin{bmatrix} f_0 & g_1 & -k_I \end{bmatrix} \begin{bmatrix} y_k \\ u_{(k-1)} \\ z_k \end{bmatrix} \quad (5)$$

k_I Is assigned a negative sign in equation (5) to allow it to take the conventional PI control law

Rewriting (5) into difference equation format gives:

$$u(k) = -f_o y(k) - g_1 u_{(k-1)} + \frac{k_1}{1 - z^{-1}}\left(y_{dk} - y_k\right)$$

The closed loop PIP representation as a block diagram can now be constructed from the information above.

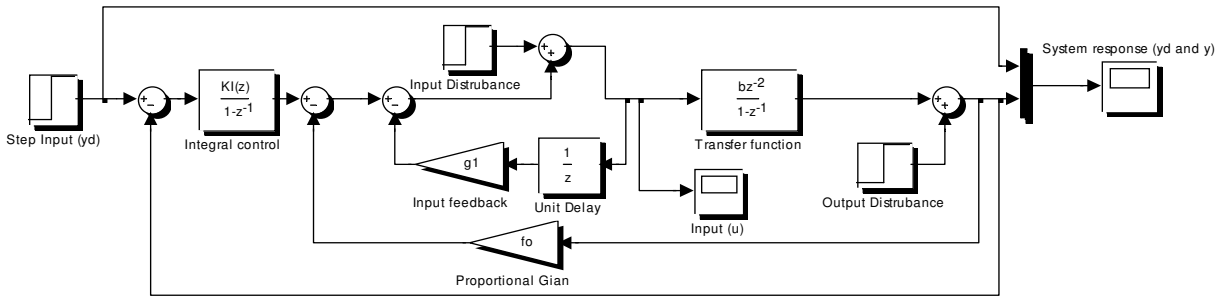

Figure (45) Simulink representation of the closed loop PIP controller for the excavator arm

Finally with the substitution of control gains into the closed loop (TF), equation (3) is defined as:

$$y(k) = \frac{k_I b_2 z^{-2}}{\left(1 - z^{-1}\right)\left[\left(1 + g_1 z^{-1}\right)\left(1 - z^{-1}\right) + \left(f_0 b_2 z^{-2}\right)\right] + k_I b_2 z^{-2}}\, y_d(k)$$

$$y(k) = \frac{k_I b_2 z^{-2}}{\left(1 - z^{-1}\right)\left[\left(1 - z^{-1} + g_1 z^{-1} - g_1 z^{-2}\right) + \left(f_0 b_2 z^{-2}\right)\right] + k_I b_2 z^{-2}}\, y_d(k)$$

$$y(k) = \frac{k_I b_2 z^{-2}}{1 - z^{-1} + g_1 z^{-1} - g_1 z^{-2} - z^{-1} + z^{-2} - g_1 z^{-2} + g_1 z^{-3} + f_0 b_2 z^{-2} - f_0 b_2 z^{-3} + k_I b_2 z^{-2}}$$

$$y(k) = \frac{k_1 B\left(z^{-2}\right)}{1 + (g_1 - 2)z^{-1} + [(f_0 + k_1)b_2 - 2g_1 + 1]z^{-2} + (g_1 - f_0 b_2)z^{-3}}\, y_d(k)$$

The characteristic equation has the following form:

$$z^3 + (g_1 - 2)z^2 + [(f_o + k_I)b_2 - 2g_1 + 1]z + (g_1 - f_0 b_2) = 0$$

The equation shows that the closed loop PIP (TF) has three poles.

6.9 Selecting the PIP model poles and gains

From the RIV models the excavator (TF) was found and the (b) parameters logged see table (39). With a discrete time system based on the Z operator (TF), for the closed loop system to be stable the system poles should have a value less than unity (1). The (TF) for the arm and boom were trailed with a range of pole assignment using the PIP function within Matlab, the control gains are computed in table (4)

Boom closed loop response average (b = 0.0015) moving up/down				
Poles	Proportional Gain	Input Feedback	Integral control	System input required
0.1	1134	1.7	486	4860
0.2	938.67	1.4	341.33	3410
0.3	751	1.1	228.67	2286
0.4	576	0.8	144	1720
0.5	416	0.5	83.33	1251
0.6	277.33	0.2	42.67	921
0.7	162	-0.1	18	648
0.8	74.67	-0.4	5.33	402
0.9	19.33	-0.7	0.67	191

Arm closed loop response average (b = 0.0054) moving up/down				
Poles	Proportional Gain	Input Feedback	Integral control	System input required
0.1	315	1.7	135	1350
0.2	260.7407	1.4	94.8148	948
0.3	208.7037	1.1	63.5185	635
0.4	160	0.8	40	480
0.5	115.7407	0.5	23.1481	347
0.6	77.037	0.2	11.8519	256
0.7	45	-0.1	5	180
0.8	20.7407	-0.4	1.4815	112
0.9	5.3704	-0.7	0.1852	53

Table (4) Log of the estimated system gains for the excavator boom and arm joints
Using an average (b) = 0.0054 and 0.0015 respectively

From observation of table (4) it maybe possible to use an overall average value of (b) to design the closed loop system for both the excavator arm and boom joint the next step in the model design is to check the model robustness.

Robustness is terminology used to assess the ability of a closed loop (TF) model. The model must be suitable for the full speed range of the system e.g. if we use a model with poles of 0.5, are the gains for this model suitable for lower

joint speeds as well as the control of faster joint speeds? As the maximum output for the joints is ±1000 table (4) is reduced see table (5) below.

Arm closed loop response average (b = 0.0054) moving up/down				
Poles	Proportional Gain	Input Feedback	Integral control	System input required
0.2	260.7407	1.4	94.8148	948
0.3	208.7037	1.1	63.5185	635
0.4	160	0.8	40	480
0.5	115.7407	0.5	23.1481	347
0.6	77.037	0.2	11.8519	256
0.7	45	-0.1	5	180
0.8	20.7407	-0.4	1.4815	112
0.9	5.3704	-0.7	0.1852	53

Boom closed loop response average (b = 0.0015) moving up/down				
Poles	Proportional Gain	Input Feedback	Integral control	System input required
0.6	277.33	0.2	42.67	921
0.7	162	-0.1	18	648
0.8	74.67	-0.4	5.33	402
0.9	19.33	-0.7	0.67	191

Table (5) is a list of the available system poles and gains

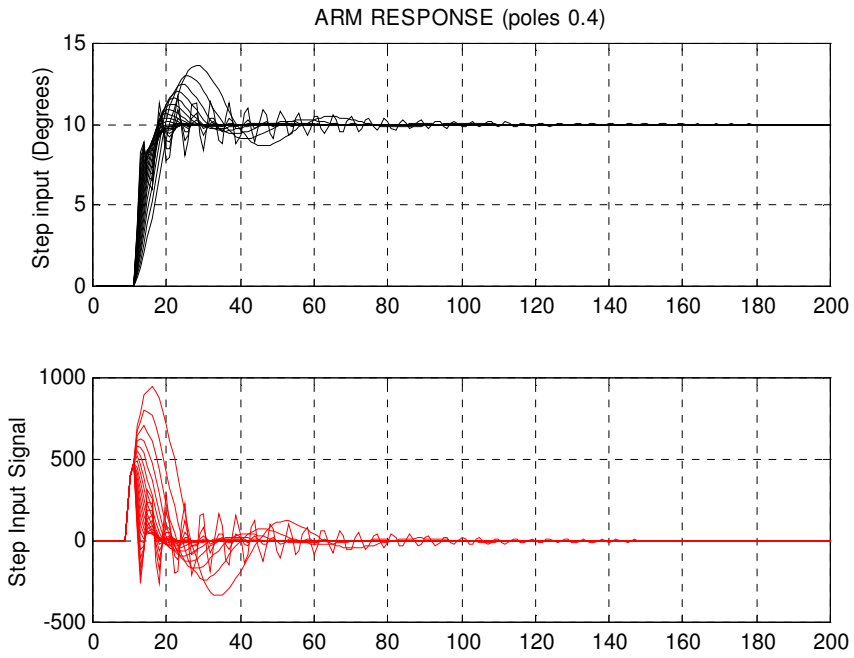

Figure (46) Excavator arm response with system pole at 0.4

Setting the system poles at (0.4) with gains found using (b = 0.0054) over the full range of arm speeds we find the system unstable with overshoot and oscillation from a step input. System poles at (0.6) generate a slower response for the arm with the same amount of overshoot as with poles at (0.4), the system reaches (SS) steady state after 140 samples in this case.

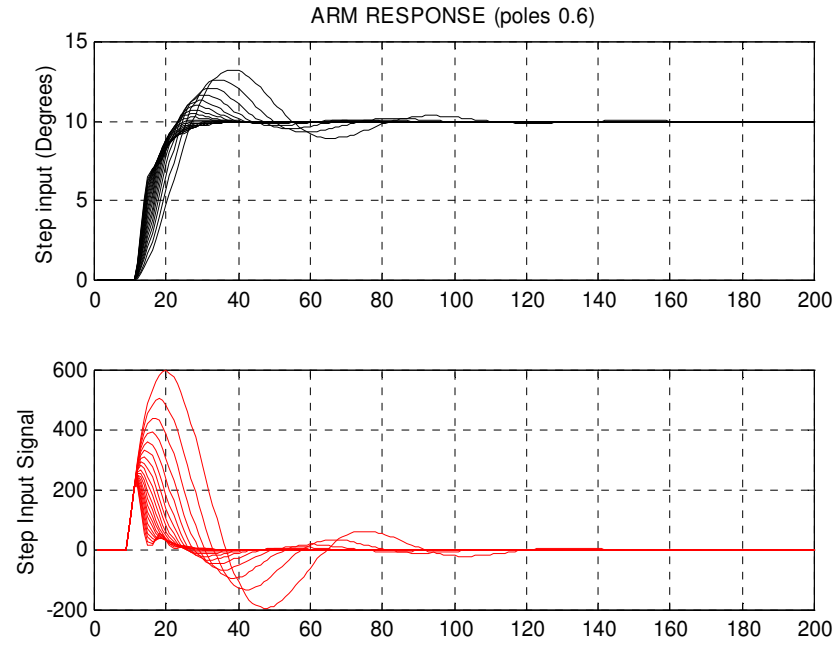

Figure (47) Excavator arm response with system pole at 0.6

From inspection of table (5) the boom has 4 different real pole values with gains to select from. Using trail and error and setting the poles at 0.6 with system gains of [277.33 0.2 42.67] the system response is pictured in figure (48).

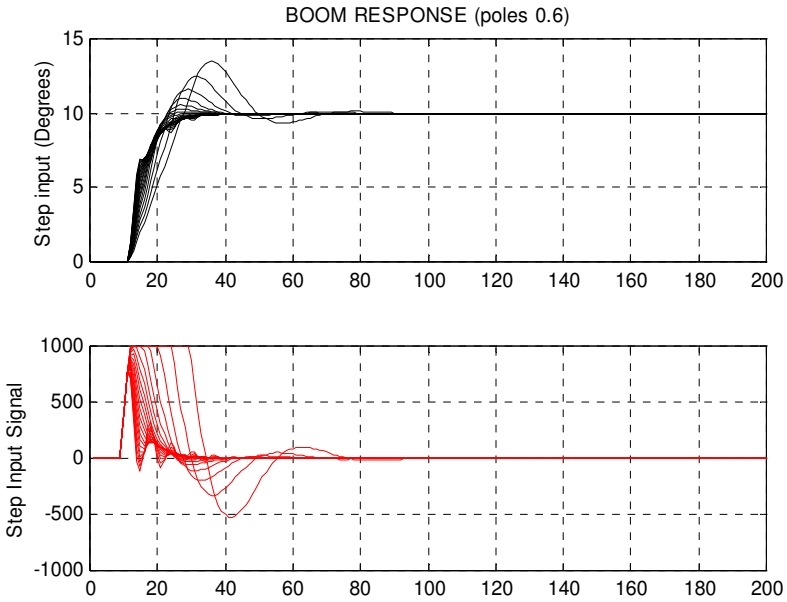

Figure (48) Excavator boom response with system pole at 0.6

Again the first trial of closed loop pole assignment is no good; the boom requires more input voltage than is available to response. Figure (49) below has the closed loop poles at 0.8 with gain [74.67 -0.4 5.33] showing a system that is stable and controllable.

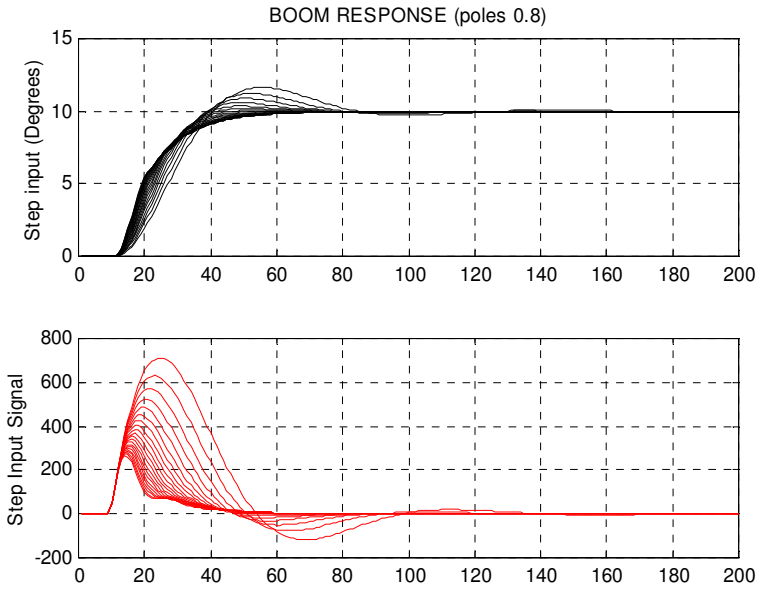

Figure (49) Excavator boom response with system pole at 0.8

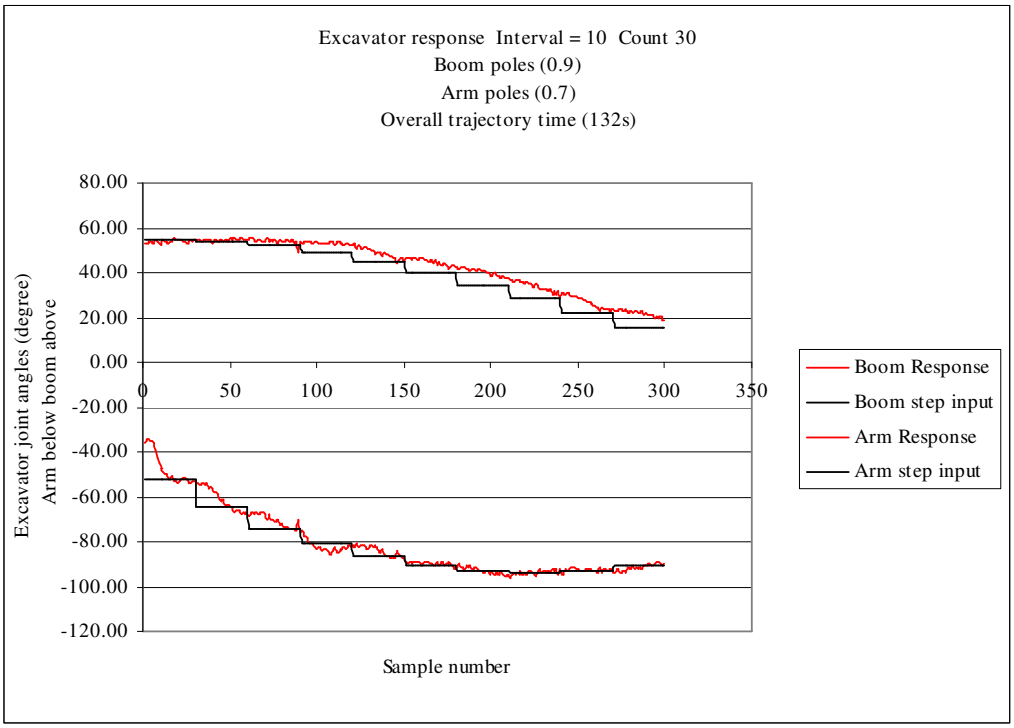

Figure (50) Excavator arm joints response for trajectory path 7.5m (10 intervals count 30)

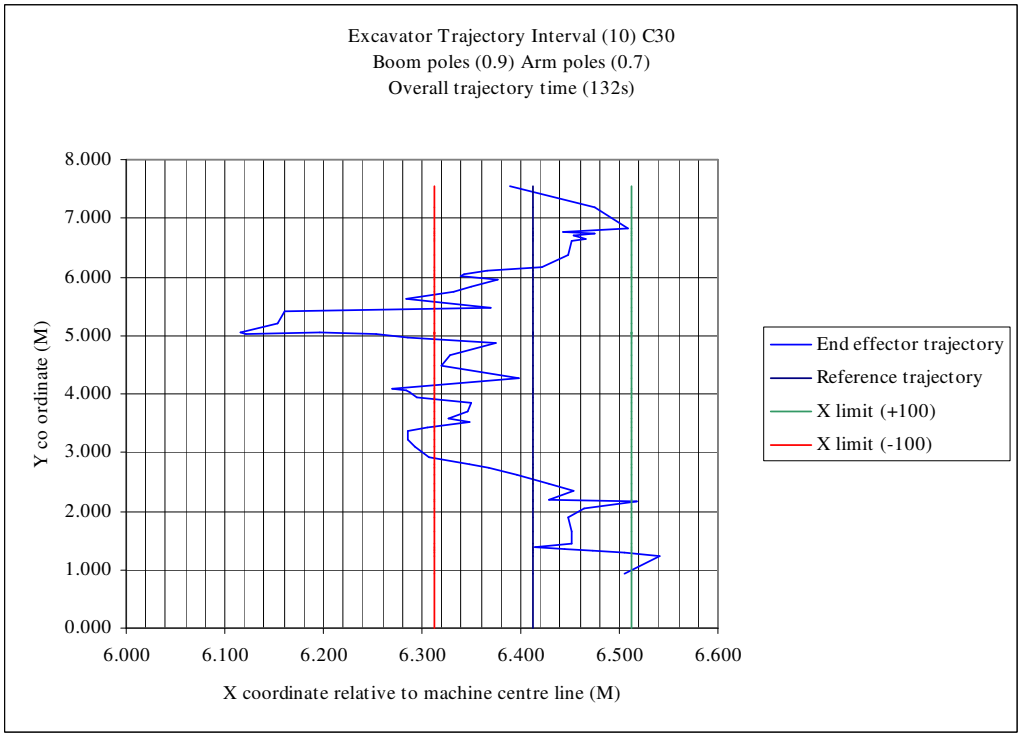

Figure (51) Excavator vibro pivotal trajectory path 7.5m (10 intervals count 30)

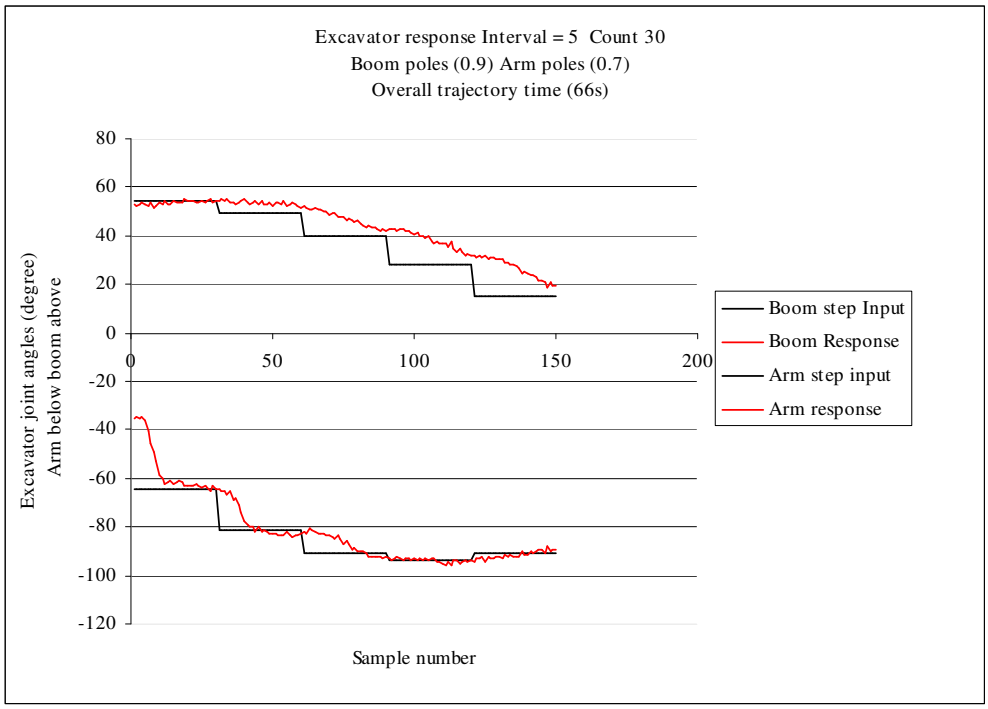

Figure (52) Excavator arm joints response for trajectory path 7.5m (5 intervals count 30)

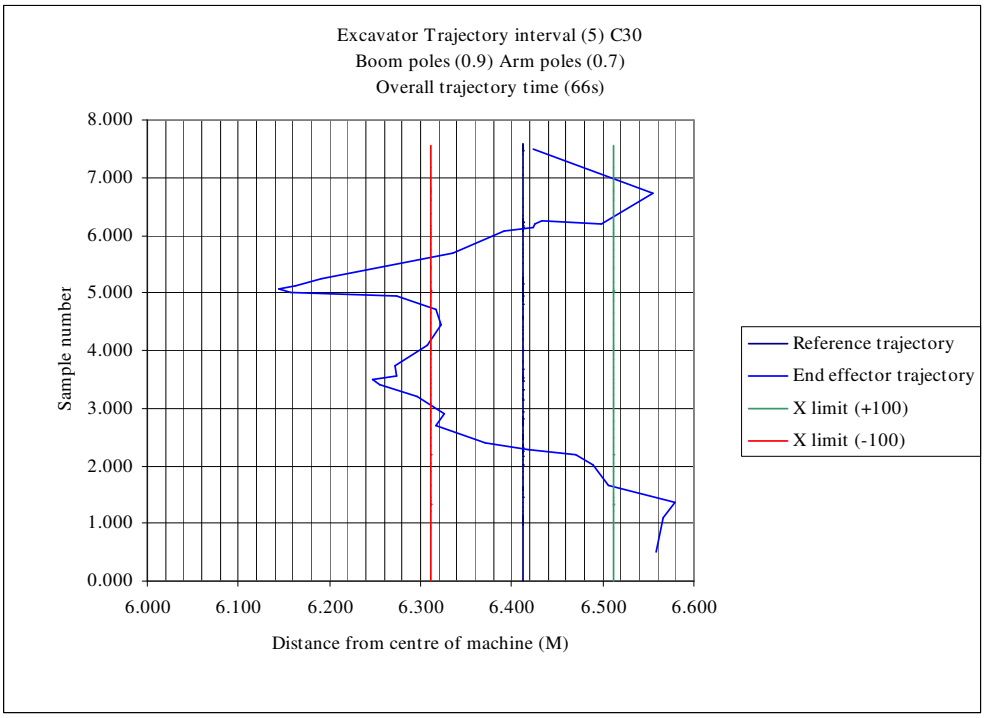

Figure (53) Excavator vibro pivotal trajectory path 7.5m (5 intervals count 30)

6.10 Excavator response

The poles and their estimated system gains for the arm and boom shown in figure (45 and 47) respectively were tested and the response of excavator observed. The controller was capable of controlling the boom but unable to control the arm with these system gains. Again using trial and error the arm was monitored with poles of (0.7) gains [45 -0.1 5]. The response although improved now made the arm slower to react. This in turn caused the arm to lag the boom in reaching the set point (interval). The next test was to try and synchronise the arm and boom by slowing down the boom and assigning it poles of (0.9) gain [19.33 -0.7 0.67]. The response of the excavator from the latter poles and gains can be seen in figures (50 > 53). Although the excavator arm was moving under control the end effector (vibro pivotal) was exceeding the objective limit of ±100 mm from the target trajectory path. The next step in the controller design was to implement a more sophisticated method of pole assignment as this crude method of trial and error to find the optimum system gains was unsuccessful.

6.11 Optimal control [8 12]

The gains of the system are found in this method of pole assignment by minimising the following cost function.

$$J = \frac{1}{2}\sum_{i=0}^{\infty} x(i)^t Q x(i) + r(u(i)^2)$$

Where:

$x = state \quad vector$

$Q = symmetric \quad weighting \quad matrix$

$r = weight \quad input$

Therefore in the case of the excavator with equal weighing on the state vector variables:

$$J = \begin{bmatrix} y_k & u_{(k-1)} & z_k \end{bmatrix} \begin{bmatrix} 1 & 0 & 0 \\ 0 & 1 & 0 \\ 0 & 0 & 1 \end{bmatrix} \begin{bmatrix} y_k \\ u_{(k-1)} \\ z_k \end{bmatrix} + ru_k^2$$

$$J = y_k^2 + u_{(k-1)}^2 + z_k^2 + ru_k^2$$

The algebraic Riccati Equation (ARE) can be used to obtain the control variables:

$$k = \left[g^T \; p^{(i+1)} \; g + r\right]^{-1} g^T \; p^{(i+1)} \; F$$

$$P^{(i)} = F^T \; P^{(i+1)} \left[F - gr\right] + Q$$

The figures below display the joint and end effector trajectory path, the initial start and endpoint remain the same as that in poles assignment, section (6.9) earlier. The charts show a greater improvement from figure (52 > 53) in the controlling of the end effector. Although at the initial interval for the arm, the joint speed needs to be increased to allow the arm to reach the set point (interval (1)) this deviation is recorded by the sensors as +75 above the limits. Although the end effector strays beyond its upper limit and its performance looks unacceptable from the graph, by visual inspection of the excavator arms motion this large deviation highlighted dramatically in figure (55) is slightly noticeable.

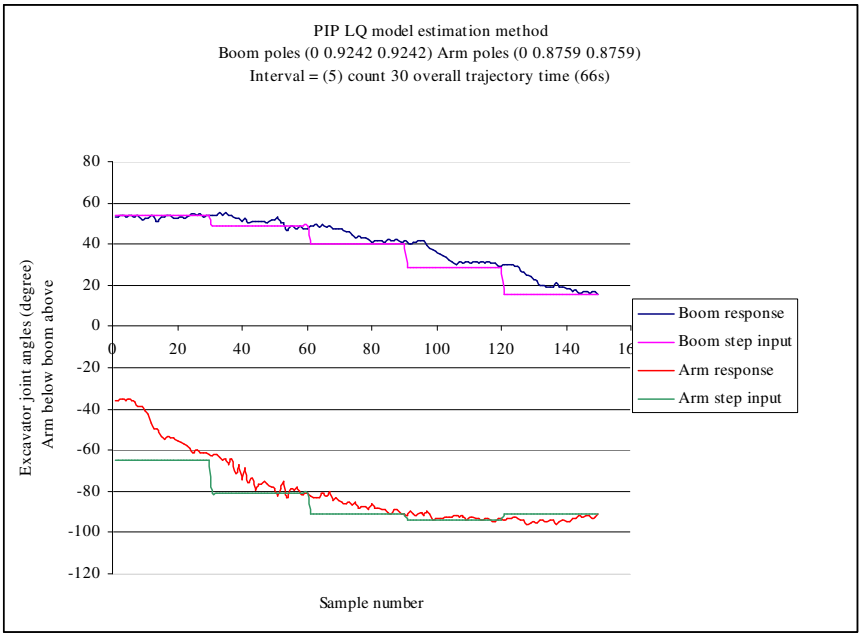

Figure (54) PIP LQ estimation for the new joint response

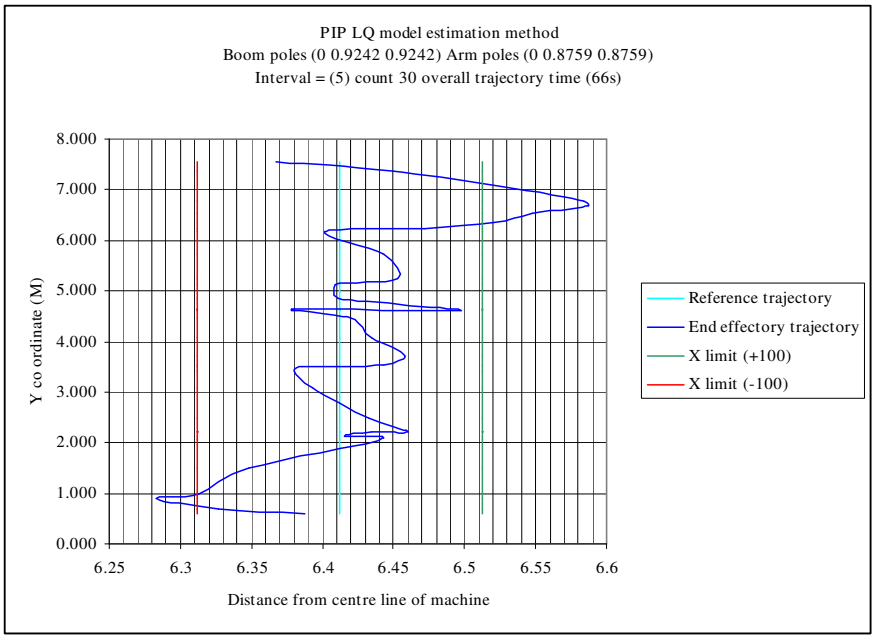

Figure (55) PIP LQ estimation for the new end effector response

Closer examination of figure (54) shows the arm and the boom reaching the set point at roughly the same time; it could therefore be assumed the joints must be travelling in synchronisation with each other.

Compared with human operators the controller is capable of manipulating the excavator arm within limits of ±100mm and in the middle region 6m downwards the controller manages to achieve tolerances ±50mm. As compared with the human operator who can average trajectory misalignment of up to ±300mm. This incorrect manipulation of the excavator arm (see section (1)) is reason for this research.

7.0 Conclusion and future work

The objective of this project was completed successful in its aim of controlling the trajectory of an excavator arm. The control of the arms speed although crude was effective; more work is needed on a controller that not only controls the positioning of the end-effector but also the velocity as it follows the trajectory path. Currently research is under way at Lancaster University for a more sophisticated non-linear controller.

Section (3.4) explains the process of selecting the excavator arm sensors, future development of this type of control should invoke the choice of sensor with a greater measuring span. The ±60º sensors implemented here have little margin for the machine to work on uneven ground as the inclinometer measure the absolute angle. It is suggested for future work to employ the use of a sensor with ±20º extra measuring span than the machines movement capabilities would be a good option.

Section (5.1) states it may be possible to control the excavator arm using the joint space trajectory method. Now the controller design is finished it is concluded, that to perform straight line trajectory, the path must invoke the use of inverse kinematics.

The controller was based on the Elan-104NC which had 100MHz AMD SC400 with 10MB of hard drive spacer. The selection of a controller with a large hard drive will help in the designing stage. All of the software needed for the controller design could be loaded onto the system and worked on locally. Whereas the programming of the Elan-104NC was time consuming in the way of uploading and download files from an external laptop .

No	Reference
[1]	www.mooreandtaber.com
[2]	www.riekerinc.com
[3]	www.Dennison.com
[4]	www.savery.co.uk
[5]	www.chproducts.com
[6]	Dynamic analysis of serial semi-elastic robot. Essam-Eldin Mohamed Shaban pp 45-49 (1997)
[7]	www.control.isy
[8]	ENGR 406 Intelligent control paper, discrete time model based control and state variable feedback, C J Taylor. (2003)
[9]	Proportional Integral Plus control of an intelligent excavator. Jun Gu, James Taylor, Derek Seward. (2004)
[10]	The Automation of piling rig positioning utilising multivariable (PIP) control. R Dixon, A Chotai, J N Scott. (1997)
[11]	Proportional Integral Plus (PIP) control of ventilation rate in agricultural buildings. C J Taylor, P Leigh, L Price, P C Young, E Vranken, D Berckman. (2004)
[12]	State dependent parameter, proportional integral plus (SDP-PIP), control of a non-linear robot digger arm E.M. Shaban, C.J. Taylor* and A. Chotai (2004)

Topic	Internet references and useful web site addresses
Hydraulic excavator	www.Liebherr.com www.ridway-holdings.co.uk www.Volvo.com www.cat.com
Hydraulic Valve blocks	www.RexrothBosch.com www.Atos.com www.Dennison.com www.savery.co.uk www.powerline@tiscali.co.uk www.riekerinc.com
Angle Sensors	www.gemac-chemnitz.de www.sensors-uk.com www.info@spectronsensors.com www.spp.co.jp www.schaevitz.com www.sentechlvdt.com www.singer-instruments.com www.balluff.co.uk www.efunda.com www.tilt-measurment.com
joystick	www.globalspec.com www.flightlink.co.uk www.chproducts.com www.bucher-hydrauilc.de www.can-cia.de
Motion controllers	www.galilmc.com www.omsmotion.com www.embedded.com www.acs-tec80.com www.dsl-ltd.co.uk www.arcom.com www.triomotion.com
PIP controller	www.es.lancs.ac.uk

Note: References listed are also useful for future developments of motion control

Number	Appendices
Annex 1	Typical Arm angle sensor bracket design
Annex 2	AIM 104 Multi / IO
Annex 3	AIM 104 Relay8/IN8
Annex 3	HFX hand grip joystick